

On the Worldsheet Theories of Strings Dual to Free Large N Gauge Theories

Ofer Aharony^{1♣}, Zohar Komargodski^{2♣} and Shlomo S. Razamat^{3♠}

♣ Department of Particle Physics, The Weizmann Institute of Science,
Rehovot 76100, Israel

♠ Department of Physics, Technion – Israel Institute of Technology,
Haifa 32000, Israel

We analyze in detail some properties of the worldsheet of the closed string theories suggested by Gopakumar to be dual to free large N $SU(N)$ gauge theories (with adjoint matter fields). We use Gopakumar's prescription to translate the computation of space-time correlation functions to worldsheet correlation functions for several classes of Feynman diagrams, by explicit computations of Strebel differentials. We compute the worldsheet operator product expansion in several cases and find that it is consistent with general worldsheet conformal field theory expectations. A peculiar property of the construction is that in several cases the resulting worldsheet correlation functions are non-vanishing only on a sub-space of the moduli space (say, for specific relations between vertex positions). Another strange property we find is that for a conformally invariant space-time theory, the mapping to the worldsheet does not preserve the special conformal symmetries, so that the full conformal group is not realized as a global symmetry on the worldsheet (even though it is, by construction, a symmetry of all integrated correlation functions).

February 2006

¹Ofer.Aharony@weizmann.ac.il.

²Zkomargo@weizmann.ac.il.

³Razamat@physics.technion.ac.il.

Contents

1	Introduction and Summary	1
2	A Recipe for the Closed String Dual of Free Gauge Theories	6
2.1	Mathematical background	6
2.2	Cell decompositions	8
2.3	Schwinger parametrization of Feynman diagrams	10
2.4	The mapping of a free field theory graph to a closed string amplitude . . .	12
3	On Worldsheet and Space-time OPEs	16
4	Sphere Diagrams	21
4.1	Three-point function on the sphere	21
4.2	The Y four-point function diagram	25
4.3	The Π four-point function diagram	29
4.4	The X five-point function diagram	32
5	Two-Point Function on the Torus	39
A	More Sphere Diagrams	47
A.1	Circular four-point function	48
A.2	Circular five-point function	50
B	A Short Primer on Elliptic Functions	54

1 Introduction and Summary

It is widely believed that large N $SU(N)$ gauge theories (with adjoint matter fields) are dual to closed string theories with a string coupling constant $g_s \sim 1/N$, in the limit of large N with fixed 't Hooft coupling $\lambda \equiv g_{YM}^2 N$. The original argument of 't Hooft for this duality [1] was based on a reinterpretation of the Feynman diagrams of the gauge theory as closed string diagrams. The Feynman diagrams may be written in 't Hooft's double-line notation, in which they can be interpreted as two dimensional surfaces with holes. It was

conjectured that there should be an equivalent description in which the holes get filled up, leading to closed Riemann surfaces without boundaries. In a normalization in which the gauge coupling constant appears only as a factor of $1/g_{YM}^2$ sitting in front of the action, the dependence of each Feynman diagram on g_{YM} and on the rank N of the gauge group is determined by the topology of its surface. A graph with V vertices and E propagators, whose topology has g handles and h holes, is proportional to

$$(g_{YM}^2)^{-V+E} N^h = (g_{YM}^2)^{-V+E-h} (g_{YM}^2 N)^h = (g_{YM}^2)^{2g-2} (g_{YM}^2 N)^h = (g_{YM}^2)^{2g-2} \lambda^h. \quad (1)$$

For any correlation function M , the sum over Feynman diagrams may then be rewritten as a sum over all topologies,

$$M = \sum_{g=0}^{\infty} \sum_{h=1}^{\infty} F_{g,h} (g_{YM}^2)^{2g-2} \lambda^h = \sum_{g=0}^{\infty} F_g(\lambda) (g_{YM}^2)^{2g-2} = \sum_{g=0}^{\infty} \tilde{F}_g(\lambda) N^{2-2g}, \quad (2)$$

where $F_g(\lambda) \equiv \sum_{h=1}^{\infty} \lambda^h F_{g,h}$, $\tilde{F}_g(\lambda) \equiv \lambda^{2g-2} F_g(\lambda)$, and the coefficients $F_{g,h}$ depend on all other coupling constants of the theory. This equation has the same form as the perturbative expansion of a closed string theory with string coupling $g_s \sim 1/N$, motivating the conjecture described above. Even though the derivation of (2) was based on perturbation theory, such an expansion is believed to exist for any value of λ .

The arguments above do not give a direct construction of the string theory dual to a specific large N gauge theory. In the beginning, the only examples of 't Hooft's conjecture were limited to field theories in two dimensions or less. This has changed in the last decade, following [2]. Now there are many examples in which it is known how to find the closed string dual of gauge theories which can be realized as the world-volume theories of D-branes in some decoupling limit⁴. In these cases⁵ the closed string dual turns out to be a standard closed string theory, living in a warped higher dimensional space. In some cases, for which the gauge theory is strongly coupled, the dual string background is weakly curved and a gravity approximation of the string theory may be used. In general (and, in particular, for all weakly coupled gauge theories), this is not the case, and the dual string theory is

⁴There are also more general dualities between open and closed string theories, which we will not discuss here.

⁵This is believed to be true also for general gauge theories, which can be reached by deformations of theories living on D-branes.

complicated (and does not necessarily have a geometrical interpretation). For standard gauge theories it is not known how to derive the duality to closed strings, though there is a lot of evidence that it is correct; in some topological cases one can provide an explicit derivation of the duality [3].

The general mapping (2) works for any value of λ , and in particular it is interesting to consider the $\lambda \rightarrow 0$ limit, for which the gauge theory has a perturbative expansion. This limit does not always make sense, since in many cases λ is related to the only scale in the theory. However, the limit $\lambda \rightarrow 0$ is expected to be smooth in many cases of four dimensional conformal gauge theories (which are conformal for every value of the gauge coupling), such as the $\mathcal{N} = 4$ supersymmetric Yang-Mills theory (dual to type IIB string theory on $AdS_5 \times S^5$), and even in other theories one can try to use (2) to define a closed string theory when λ is strictly equal to zero⁶. Indeed, the correlation functions of free gauge theories (with $g_{YM} = 0$) have a topological expansion of the form (2) in powers of $1/N^2$, and it is interesting to ask what is their closed string dual⁷. Note that in this limit the closed string coupling must be identified with $1/N$ rather than with the vanishing g_{YM} (even though D-brane constructions usually give $g_s \propto g_{YM}^2$). Clearly, given a dual to the free gauge theory, one can map the interaction vertices in space-time to interactions on the worldsheet (by the mapping of gauge-invariant operators in space-time to integrated vertex operators on the worldsheet), and rewrite the perturbative expansion in λ of the space-time gauge theory as a perturbative expansion in λ on the worldsheet.

There have been various proposals for how to study the string dual of free large N gauge theories (see, for instance, [5, 6, 7, 8, 9, 10, 11, 12, 13]). It is clear that the dual string theories must live in a highly-curved background, which may or may not have a geometrical interpretation (for four dimensional free gauge theories with massless adjoint fields, which are conformally invariant, one expects that any geometrical interpretation

⁶Of course, the free gauge theory does not have confining strings, which were one of the original motivations for 't Hooft's proposal. However, following the AdS/CFT correspondence, it was recognized that confinement is not a necessary feature for a dual string theory to exist. Compactified free gauge theories do exhibit a deconfinement phase transition and a Hagedorn spectrum [4].

⁷Of course, we are discussing here correlation functions of local gauge-invariant operators such as $\text{Tr}(F_{\mu\nu}^n)$, and not the S-matrix which is the identity matrix in the free gauge theory. These are expected to be the correct observables for gauge theories and for their string theory duals.

should include an AdS_5 factor). In this paper we will study in detail a specific proposal by R. Gopakumar [11] for how to map the Feynman diagrams to worldsheets⁸. This proposal is based on rewriting the propagators in the Feynman diagrams as integrals over Schwinger parameters, and mapping these parameters to the moduli of a Riemann surface with holes (which include the moduli of the closed Riemann surface, plus the circumferences of the holes). One can then integrate over the parameters of the holes, and translate any Feynman diagram to a correlation function on the string worldsheet. We will focus on the special case of correlation functions of gauge-invariant operators involving adjoint scalar fields in four dimensional free gauge theories, but the conclusions apply more generally, to any local gauge-invariant operators in any free gauge theory.

The mapping of [11] (which we review below) gives a closed string theory whose integrated correlation functions (of physical vertex operators), by construction, reproduce the space-time correlation functions. The worldsheet theory is also automatically conformally invariant (so that it can be interpreted as a closed string theory in conformal gauge) and modular invariant. However, the construction does not give a Lagrangian for the worldsheet theory, and it is not clear from the construction if this worldsheet theory is a standard local conformal field theory or not.

In this paper we will note two strange properties of the worldsheet correlation functions resulting from Gopakumar's prescription. The first is that, for some Feynman diagrams, the correlation functions turn out to be non-vanishing only on a sub-space of the moduli space. The dimension of the moduli space for a closed string n -point function at genus g is $2n + 6g - 6$, and in some cases we find that the locus on which the correlation function is non-vanishing has a lower dimension. For example, for a particular planar 4-point function, we find that it is non-vanishing only when all four points lie on a line. Obviously, such a result is not consistent with the usual analyticity properties of correlation functions in local field theories (such as having operator product expansions at small distances). There are (at least) three possible explanations of this result : (a) Gopakumar's prescription is wrong; (b) The worldsheet theory is non-local, and its correlation functions are not analytic; (c) There are global contributions to correlation functions (in addition to the local ones), coming for instance from zero modes on the worldsheet, which cause the correlation

⁸This proposal was further studied in [14].

functions to vanish in many circumstances. We will not be able to determine which of these interpretations is correct – this is an interesting topic for further research.

A second strange property involves the space-time symmetries. Apriori one would expect that any (global) symmetry of the space-time theory should be realized as a symmetry of the worldsheet theory, which does not act on the worldsheet coordinates. For example, in the AdS/CFT correspondence, both global symmetries and the conformal symmetry in space-time map to global symmetries on the worldsheet (often related to isometries of a sigma model). Gopakumar’s prescription guarantees that any space-time symmetries will be present in the integrated correlation functions, but it does not guarantee that they will act locally on the worldsheet. We will find that, for conformally invariant theories, the mapping preserves the Poincaré and scaling symmetries, but not the special conformal transformations. These transformations are not manifestly preserved by the mapping, and by explicit computations we show that they are not symmetries of the worldsheet correlation functions (at fixed positions on the worldsheet). Thus, it seems that (unlike in the AdS/CFT correspondence) the Poincaré and scaling symmetries are realized as global symmetries on the worldsheet, but the special conformal symmetries are not. It would be interesting to investigate possible modifications of Gopakumar’s prescription in which the special conformal transformations would also act locally on the worldsheet (this may require a different choice of gauge for the worldsheet diffeomorphisms than the one implied by the mapping of [11], just like Lorentz transformations do not act locally in light-cone gauge and space-time supersymmetry does not act locally in the NSR superstring formulation).

On the more positive side, we investigate in detail the operator product expansion (OPE) on the worldsheet, resulting from specific correlation functions in the limit where two points on the worldsheet approach each other. As mentioned above, in some cases this OPE is ill-defined because the correlation functions are non-vanishing only at special positions, but in other cases the correlation functions are non-zero when the two points approach each other, so one can check if they have an OPE expansion. We find that, in such cases, there is indeed a sensible OPE expansion, as expected from a standard local worldsheet theory. We compute the worldsheet dimensions of the operators appearing in the OPE, we show that they are consistent with a local conformal field theory (namely, they have integer values of $h - \bar{h}$), and we show that consistent results emerge from different

correlation functions (of the same operators). This may be viewed as support for option (c) above, that the conformal worldsheet theory is a standard local theory, but with some global contributions to its correlation functions.

We begin in section 2 by reviewing Gopakumar’s mapping from Feynman diagrams to worldsheets in detail. The mapping involves Strebel differentials, and we review what these are and how they are related to the moduli space of Riemann surfaces with holes. We also discuss the strange properties noted above. Section 3 is a general discussion of our expectations about space-time and worldsheet OPEs for free gauge theories and their string duals. In section 4 we discuss in detail several examples of planar correlation functions, with three, four, and five vertices. We show how to map the Feynman diagrams to worldsheet correlation functions (by computing the relevant Strebel differentials) and analyze their OPE expansions. In section 5 we perform a similar analysis for the two-point function on the torus. In appendix A we provide a few more examples of planar correlation functions, for which we were not able to perform the full computation. Finally, in appendix B we review some properties of elliptic functions which are used in section 5.

2 A Recipe for the Closed String Dual of Free Gauge Theories

2.1 Mathematical background

The nuts and bolts of Gopakumar’s proposal rely on the mathematical theory of Strebel differentials, and in particular on a theorem by K. Strebel which we describe below⁹. Let X be a Riemann surface. A quadratic differential is an expression of the form $q = \phi(z)dz^2$, which is a section of the bundle $T_X^{\mathbb{C}} \otimes T_X^{\mathbb{C}}$ (it may have poles for marked surfaces). Given such a differential, we call a curve $\gamma(t)$ horizontal if it satisfies $\phi(\gamma(t))(\gamma'(t))^2 > 0$. Similarly, a vertical curve satisfies $\phi(\gamma(t))(\gamma'(t))^2 < 0$. The prime denotes differentiation with respect to the affine parameter of the curve. The horizontal curves have an interesting behavior near the zeros and poles of ϕ . At a zero of order m there are $m + 2$ horizontal curves intersecting. At a simple pole there are no locally intersecting horizontal curves. Near a

⁹Strebel differentials are useful also in closed string field theory [15, 16].

pole of second order, one can locally write

$$\phi(z)dz^2 \simeq -\frac{p^2}{(2\pi)^2 z^2} dz^2. \quad (3)$$

To classify the horizontal and vertical curves, we note that the circular curves

$$\gamma(t) = r_0 e^{it}, \quad t \in [0, 2\pi) \quad (4)$$

are horizontal near $z = 0$, while straight lines emanating from the pole,

$$\gamma(t) = t e^{i\theta}, \quad t \in \mathbb{R}_+ \quad (5)$$

are vertical near $z = 0$. Thus, locally around any pole of second order the geometry is that of a semi-infinite cylinder.

From here on we will focus on the horizontal curves, whose global structure may in general be very complicated. It is customary to distinguish the *closed* simple horizontal curves from the other horizontal curves, and to call the complimentary set to the closed simple horizontal curves the set of critical curves (in particular, these are the curves that go through the intersection points at the zeros of ϕ). The set of critical curves for a general second order differential is very complicated and not much is known about it. Here the notion of a Strebel differential is important. Let there be n marked points x_1, \dots, x_n on our compact Riemann surface X . A *Strebel differential* q is a second order meromorphic differential which satisfies the following requirements :

- q is holomorphic on $X \setminus \{x_1, \dots, x_n\}$,
- q has a pole of second order at each x_i ,
- The set of critical curves of q is compact and of measure zero.

Now we are ready to quote the theorem of K. Strebel (for proofs and more details see [17, 18, 19]). Assigning a positive number p_i to each marked point x_i , the theorem states that there is a unique Strebel differential with double poles of residues p_i at the points x_i . Equivalently, we require $\oint_{x_i} \sqrt{q} = p_i$, where the integration is on a horizontal closed curve (close enough to the double pole) and the branch cut is chosen so that the integral is positive with respect to the orientation specified by the complex structure. The space of

possible X 's with n marked points and a positive number p_i at each marked point is called the decorated moduli space of Riemann surfaces, $\mathcal{M}_{g,n} \times \mathbb{R}_+^n$, where g is the genus of X . The theorem provides a unique Strebel differential for any point on this moduli space.

The conclusions above can be carried further to establish a more useful (for us) isomorphism between the (equivalence classes of the) space of graphs with a prescribed length to each edge and the decorated moduli space. It follows from the definitions above that the set of critical curves of any Strebel differential is a graph. Given the critical graph, we assign a length to each edge of the critical graph by the integral along the edge $\int_{z_1}^{z_2} \sqrt{q}$, where the integral is performed in the orientation for which it is positive (the integrand is real since the curve is horizontal). Note that z_1 and z_2 are zeros of q , and the integral is carried over the critical curve, although the result for any homotopic curve is the same (correctly dealing with the branch cuts). Using Strebel's theorem, this gives a mapping from the decorated moduli space to graphs with edge lengths. The opposite mapping, gluing a graph with given edge lengths to form a specific Riemann surface, is a bit more intricate and is described in the references above.

2.2 Cell decompositions

In this subsection we show how the above results give rise to cell decompositions of X and of the decorated moduli space.

Firstly, the unique Strebel differential on a specific marked Riemann surface X induces a cell decomposition of X in the following manner. One collects all vertices of the critical graph (which are the zeros of q) in the 0-cell part of the complex. The 1-cells are the edges of the critical graph, and finally, the 2-cells are the domains around the poles, which are foliated by the closed simple horizontal curves. This gives a cell decomposition because the domains around the poles are conformal to disks. In particular, one may define a new holomorphic coordinate w_i around each x_i such that the differential in the whole domain foliated by the closed simple horizontal curves is given exactly by

$$q = -\frac{p_i^2}{(2\pi)^2 w_i^2} dw_i^2. \quad (6)$$

Of course, the Euler formula $v - e + f = 2 - 2g$ is satisfied, where v is the number of 0-cells, e is the number of 1-cells and f is the number of 2-cells. Figure 1, copied from [16], shows

this decomposition for the case of four punctures on the sphere (conformally mapped to the plane with the punctures at $0, 1, \xi, \infty$).

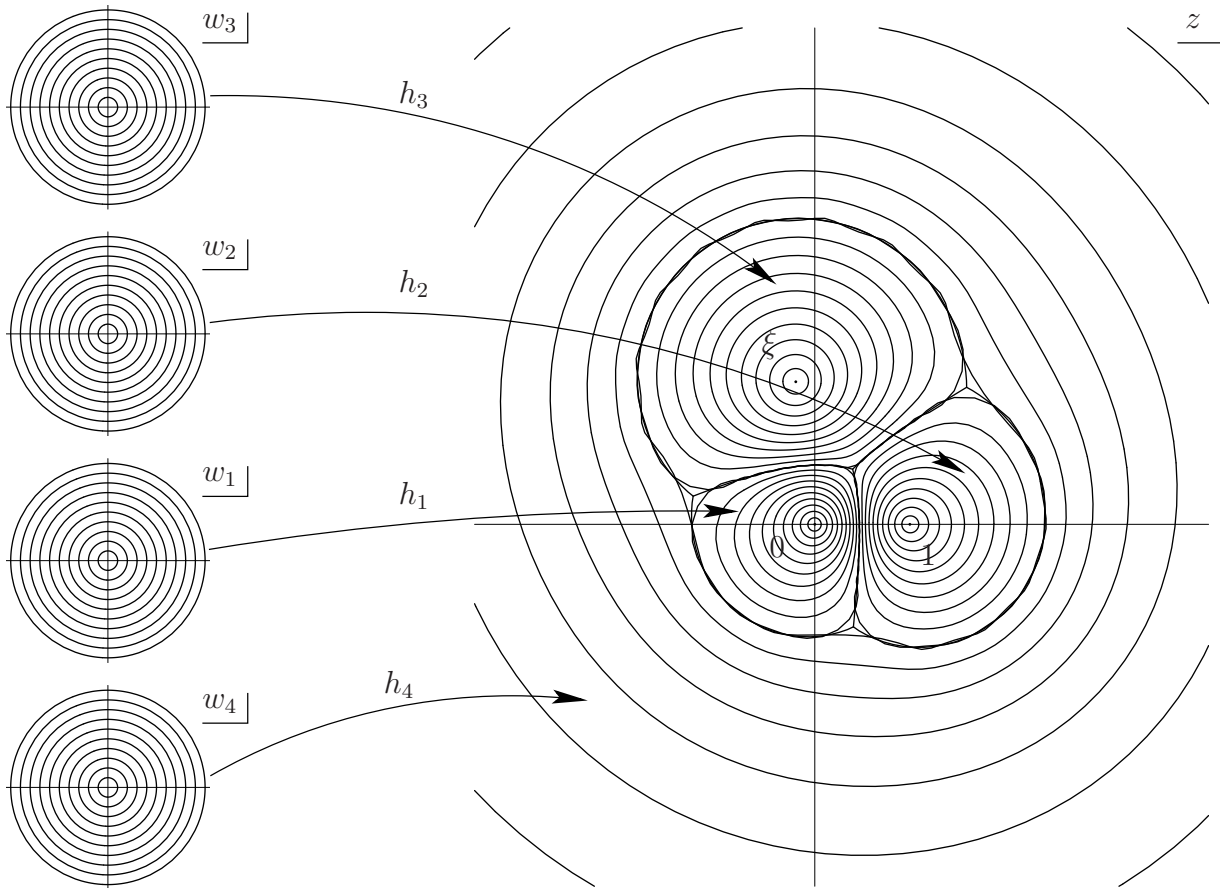


Figure 1: The horizontal curves for a four-punctured sphere. Each domain is conformally a disk. The critical graph is easily seen. This figure was produced by a numerical analysis which is described in [16].

Secondly, the isomorphism of the decorated moduli space with the metric graphs induces a cell decomposition of the decorated moduli space. It is clear that any vertex of order higher than 3 in the critical graph can be split in various channels until the graph has only vertices of order 3. This can be done without intersecting other edges or affecting the genus. Hence, a generic Riemann surface is mapped to a Strebel differential which has at most simple zeros. Consequently, these trivalent graphs sweep out a top dimensional cell of the decorated moduli space. Riemann surfaces which map to graphs with higher order vertices (coming from at least two zeros that have merged) are part of some lower

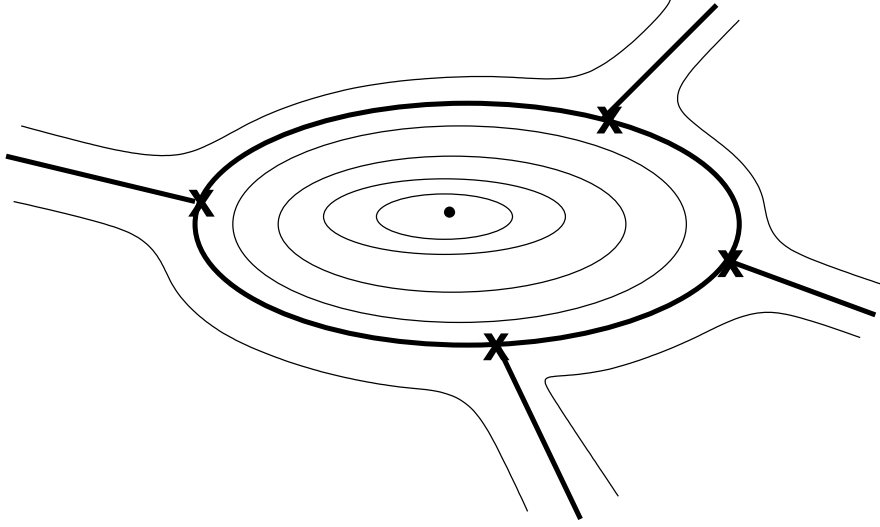


Figure 2: (borrowed from [11]) A characteristic ring domain in the vicinity of a double pole (marked with a dot). The non-closed horizontal trajectories are shown by thick lines. These begin and end at zeros marked by a cross.

dimensional cell in the complex. It can be shown that this description is compatible with the continuity notion on the decorated moduli space, and hence can be viewed as a cell decomposition. This result has had many applications both in mathematics and in physics. Some are summarized in the references of [11] (see especially the Kontsevich theory [20]).

2.3 Schwinger parametrization of Feynman diagrams

As described in the introduction, we wish to map the Feynman diagrams of a free gauge theory to closed string diagrams, namely to punctured Riemann surfaces. It is quite clear that the critical graph itself is not similar in any way to the typical Feynman graph of a free gauge theory (where we put composite operators such as $\text{Tr}(F_{\mu\nu}^n)$ as insertions). Indeed, in the vicinity of some second order pole the critical graph would generically look like Figure 2. This is not adequate to describe a subgraph of a free gauge theory diagram; rather, this seems to describe vacuum-vacuum transitions in some theory with a cubic interaction term and elementary fields in the adjoint representation (such as the Kontsevich matrix model [20]). To figure out how to recast free gauge theory graphs in this form we make a detour in this subsection to introduce the Schwinger parametrization of Feynman diagrams.

For simplicity, we will discuss only correlation functions of operators involving adjoint scalar fields Φ , of the form $\langle \text{Tr}(\Phi^{i_1}(x_1)) \text{Tr}(\Phi^{i_2}(x_2)) \cdots \text{Tr}(\Phi^{i_n}(x_n)) \rangle$. A Euclidean propagator with momentum p of a scalar field of mass m can be rewritten as an integral over the Schwinger parameter τ of the propagator,

$$\frac{1}{p^2 + m^2} = \int_0^\infty d\tau e^{-\tau(p^2 + m^2)}. \quad (7)$$

It is usually easier to compute free field theory correlation functions in position space rather than in momentum space, since there are no integrations required in position space. The propagator in position space from x_i to x_j is the Fourier transform of (7). For the special case of massless scalar fields in four dimensions (which we will focus on for the rest of this paper, though the generalization to any other fields should be straightforward), it is simply given by (up to a constant)

$$\frac{4}{(x_i - x_j)^2} = \int_0^\infty d\sigma e^{-\sigma(x_i - x_j)^2/4}, \quad (8)$$

where $\sigma \equiv 1/\tau$ is the inverse Schwinger parameter. In order to avoid divergences, we do not consider lines that begin and end on the same vertex (so our operators will be normal ordered). A general Feynman diagram is given by a product of such factors over all the propagators in the diagram – if the k 'th propagator in the Feynman diagram ($k = 1, \dots, E$) connects x_{i_k} with x_{j_k} , the amplitude is given (up to a constant) by

$$\int \prod_{k=1}^E d\sigma_k e^{-(x_{i_k} - x_{j_k})^2 \sigma_k / 4}. \quad (9)$$

As noted in [11], any two homotopic edges in the Feynman diagram can be combined into an integral over an effective Schwinger parameter satisfying

$$\frac{1}{\tau_{eff}} = \frac{1}{\tau_1} + \frac{1}{\tau_2} \quad \text{or} \quad \sigma_{eff} = \sigma_1 + \sigma_2. \quad (10)$$

This is the well-known analogy to electrical networks (it is most easily understood by inspection of (9) where the integrand manifestly depends only on the sum of σ 's for homotopic lines). Thus, we can collapse all homotopic lines to a single line, but with a modified dependence on the effective Schwinger parameters (following from (10)). Such reduced diagrams will be named skeleton graphs. Note that the notion of homotopy is well defined

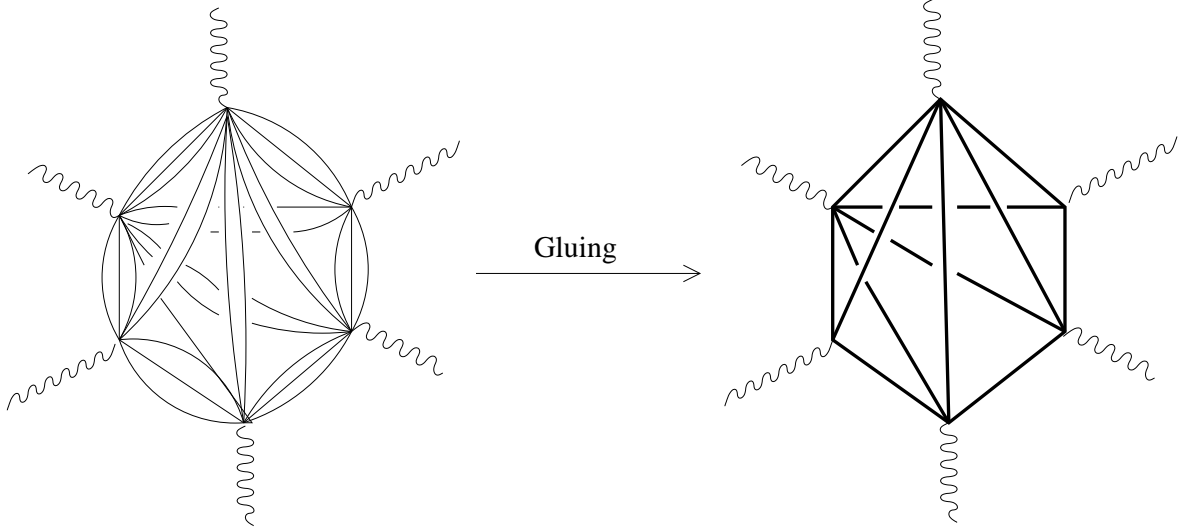


Figure 3: (borrowed from [11]) A specific (planar) 6-point diagram is reduced to a skeleton graph by collapsing color loops which are homotopic to a line.

after the diagram is drawn on some Riemann surface, or alternatively is given in double line notation where loops that respect the color flow are apparent. Strictly speaking, in a gauge theory with adjoint matter we can also combine lines in this way for non-homotopic lines between the same pair of points, but this is not useful for reasons that will become clear below. The resulting formula for the amplitude, if we have \tilde{E} reduced edges, with the r 'th edge (connecting x_{i_r} and x_{j_r}) coming from joining together m_r homotopic lines, such that its Schwinger parameter is $\tilde{\sigma}_r = \sum_{\mu_r=1}^{m_r} \sigma_{\mu_r}$, is (up to a constant depending on the m_r)

$$\int \prod_{r=1}^{\tilde{E}} d\tilde{\sigma}_r \tilde{\sigma}_r^{m_r-1} e^{-(x_{i_r}-x_{j_r})^2 \tilde{\sigma}_r/4}. \quad (11)$$

Pictorially, this procedure looks like (it is not easily drawn for some non-planar diagrams) Figure 3.

2.4 The mapping of a free field theory graph to a closed string amplitude

Now we are ready to describe the mapping from a free field theory graph to a closed string graph, by recasting the integrals over the Schwinger parameters into integrals over

the decorated moduli space of Riemann surfaces. The “skeleton reduction” procedure reviewed above suggests that the generic field theory Feynman diagram may be viewed as a triangulation of the appropriate surface. Since the critical graphs were generically trivalent, it is natural to conjecture that the rearrangement into integrals over the moduli space of Riemann surfaces should go through graph duality. In particular, the field theory insertions which are the vertices of the Feynman graph should map to poles of second order in the differential, which are faces of the critical graph, and the faces of the Feynman graph should map to the zeros of the differential. Each edge of the Feynman diagram, associated with an effective Schwinger parameter τ_i , is mapped by the graph duality to an edge of the critical graph of length l_i . Gopakumar’s suggestion for the mapping was to identify l_i with $1/\tau_i = \sigma_i$. This maps the integration over Schwinger parameters in the amplitude (11) to an integration over the space of graphs with edge lengths, which can then be mapped to an integration over the decorated moduli space. This can then be identified as a closed string amplitude (after the integration over the parameters p_i associated with the circumferences of the holes), and the procedure described above can be used to write down the integrand (the worldsheet correlation function) in this amplitude.

It is obvious from the construction that the parameters on both sides match. As we noted, by skeleton reduction the most generic field theory diagram reduces to some triangulation of the Riemann surface it lives on, so the dual graph will consist of trivalent vertices. By Euler’s theorem (applied to the dual graph), $v - e + f = 2 - 2g$ where v , e , f are the numbers of vertices, edges, and faces respectively. For the case of trivalent vertices $e = \frac{3}{2}v$. In the dual graph, f is the number of field theory insertions. So, we denote $f \equiv n$ and we obtain that the number of lengths that we integrate over is

$$e = 6g - 6 + 3n = 6g - 6 + 2n + n. \quad (12)$$

As is well known, $6g - 6 + 2n$ is the number of real moduli for a Riemann surface of genus g with n insertions (note that for $g \leq 1$ one has to saturate with the right number of vertex operators needed by the order of the conformal Killing group to use the above formula). The additional n that we obtained corresponds to the moduli p_i of the decoration, \mathbb{R}_+^n .

It is clear that the worldsheet theory which is dual to a free gauge theory must have some strange properties. For instance, a given correlation function in a free gauge theory

only gets contribution from a finite number of Feynman graphs whose genus is bounded by $g \leq g_0$, so the corresponding worldsheet correlation functions must vanish on all Riemann surfaces of genus $g > g_0$. This is a generic property of any mapping of free field Feynman diagrams to Riemann surfaces. However, the specific mapping suggested by Gopakumar also has some other strange properties. As we noted, generic Feynman diagrams (with many edges) will map to generic points on the decorated moduli space. However, in specific correlation functions one could get contributions also from less generic diagrams that have less edges. On the dual graph side such diagrams correspond to joining together several zeros of the Strebel differential, so they are localized on subspaces of the decorated moduli space. In particular, for some correlation functions the only contributions come from non-generic graphs. For example, consider the correlation function (involving a single adjoint scalar field) $\langle \text{Tr}(\Phi^2(x_1)) \text{Tr}(\Phi^2(x_2)) \cdots \text{Tr}(\Phi^2(x_n)) \rangle$. The only connected Feynman diagrams here are circular graphs which have the topology of a sphere, n vertices and n edges, so the dual graph has $f = e = n$ and $v = 2$. This Feynman diagram is mapped by Gopakumar's mapping to an n -dimensional subspace of the decorated moduli space, which is (for $n \geq 3$) of dimension $-6 + 3n$. Moreover, for $n > 6$ this subspace has a lower dimension than the moduli space of marked spheres itself (of dimension $2n - 6$), so even after we integrate over the hole sizes p_i , the corresponding amplitude will vanish for generic insertion positions, and will only be non-vanishing for specific insertion positions. This is quite surprising, since one would think that the correlation functions on the worldsheet should be smooth functions of the insertion positions. We will encounter several more examples of this phenomenon below. Even generic correlation functions, for which there are contributions from generic Feynman graphs, could have contributions also from graphs with less edges, and these contributions would give non-smooth worldsheet correlation functions as described above.

It is clear that an identification of the string theory dual of free gauge theories, of the type described above, can straightforwardly be generalized to any order in perturbation theory, simply by identifying the string theory duals of the interaction vertices in the space-time theory and adding them to the worldsheet action. Obviously, at any finite coupling a specific correlation function gets contributions involving any number of interaction vertices, so the strange properties described above would disappear. This may suggest that the limit

of taking the gauge coupling constant to zero is a singular limit, but one can still hope that it might be possible to understand the corresponding worldsheet theory.

Note that in our definition of free field theory correlation functions above we assumed that the operators are all normal-ordered; this is necessary for all correlation functions to be finite (and for preserving conformal invariance in the case of four dimensional gauge theories). However, the mapping described above from decorated Riemann surfaces to Feynman graphs gives generic Feynman graphs, which can include also self-contractions (propagators from a vertex to itself), as long as these self-contractions are topologically non-trivial (they go around another insertion or around a non-contractible curve of the Riemann surface). Again, this will result in large regions of the decorated moduli space on which the correlation functions on the worldsheet will vanish (since the corresponding field theory Feynman diagrams are set to zero). We will see explicit examples of this below.

Finally, we wish to describe another peculiar feature of the mapping described above from Feynman diagrams to worldsheets. It is natural to expect the worldsheet theory to respect all the symmetries of the space-time theory. In particular, the worldsheet vertex operators should transform under the Poincaré group in the same way as the corresponding space-time operators. And indeed, the mapping described above satisfies this property, since the Schwinger parameters (which can be thought of as proper times along the propagators) are Poincaré-invariant, so a Poincaré transformation does not change the (decorated) moduli. Next, let us assume that the space-time theory is invariant under scaling transformations $x \rightarrow \alpha x$ (as is the case for a free gauge theory with massless matter fields). Under a scaling transformation the Schwinger parameter τ transforms as $\tau \rightarrow \alpha^2 \tau$. This means that the hole radii p_i are not invariant under dilatations, because the hole radii are given by the appropriate circumferences (which are linear combinations of σ_j 's). However, note that any Strebel differential, multiplied by a positive constant, is still a Strebel differential on the same Riemann surface. Thus, the scaling transformation in space-time will act on the decorated moduli space just by multiplying the Strebel differential by a constant, and in particular the Riemann surface moduli are invariant (note that this implies that these moduli depend only on ratios of Schwinger parameters). Hence, the worldsheet vertex operators are expected to have well defined scaling transformations. Now, let us consider special conformal transformations (which are symmetries of four dimensional free gauge

theories with massless matter fields). The special conformal transformation generated by the inversion $x^\mu \rightarrow x^\mu/x^2$ acts in a more involved way on the Schwinger parameters. The propagator (for massless four dimensional scalar fields) from x_i to x_j is given by the expression $\int d\sigma e^{-\sigma(x_i-x_j)^2/4}$, so in order for it to transform properly under inversion we need to take $\sigma \rightarrow x_i^2 x_j^2 \sigma$. The formulas relating the Schwinger length parameters to the Riemann surface moduli are not invariant under such a transformation (since each Schwinger length transforms in a different way). Thus, the special conformal transformations act non-trivially on the Riemann surface moduli and not just on the vertex operators, and we do not expect to have well defined transformation laws of worldsheet vertex operators under special conformal transformations. This will be shown explicitly below. Note that this implies that the full conformal group is not realized as a global symmetry of the worldsheet theory, but only its subgroup including the Poincaré and scaling transformations.

3 On Worldsheet and Space-time OPEs

In this section we discuss our expectations about the worldsheet OPEs in the string theory which is dual to a free large N gauge theory, and their possible relations to the space-time OPEs. For simplicity we write down formulas which are correct for $d = 4$, but the generalization to other dimensions is straightforward.

The space-time OPEs in free gauge theories are rather trivial. If we just had a theory of (say) a free scalar field ϕ , the OPE of $\phi(x)$ with $\phi(y)$ would contain a single singular term of the form $I/|x-y|^2$ (where I is the identity operator), and non-singular terms of the form $(x-y)^n(\phi\partial^n\phi)(y)$ for $n = 0, 1, \dots$. In a gauge theory the OPE is slightly less trivial because we need to look only at gauge-invariant operators. For example, consider a scalar field Φ in the adjoint representation of $SU(N)$. The gauge-invariant operators we can make out of this field include $\text{Tr}(\Phi^n(x))$ for $n \geq 2$ (in the large N limit all these operators are independent), traces of products of Φ 's which include derivatives, and multi-trace operators which are products of these traces. The OPE of an operator $\text{Tr}(\Phi^{n_1}(x))$ with $\text{Tr}(\Phi^{n_2}(y))$ takes the form (as $x \rightarrow y$)

$$\text{Tr}(\Phi^{n_1}(x)) \text{Tr}(\Phi^{n_2}(y)) \sim \sum_{n=|n_1-n_2|}^{n_1+n_2} C_{n_1,n_2,n} |x-y|^{n-n_1-n_2} \text{Tr}(\Phi^n(y)) + \text{other operators}, \quad (13)$$

where the “other operators” include both operators with derivatives and multi-trace operators. In the large N limit, the coefficients $C_{n_1, n_2, n}$ have an expansion in powers of $1/N^2$, corresponding to the genus of the free-field diagrams contributing to the three-point functions represented in (13) (when they are written in ’t Hooft’s double-line notation [1]). Note that the space-time dependence of the OPE coefficients is determined by the dimensions of the participating operators, since the free gauge theory is scale-invariant.

As discussed above, we expect that the free large N gauge theory should have a string theory dual with a string coupling scaling as $1/N$, in which each of the single-trace operators of the gauge theory $\mathcal{O}(x)$ should be represented by a vertex operator on the worldsheet $V_{\mathcal{O}}(x; z)$ (we will use x, y to denote space-time positions and z, w to denote worldsheet positions). We do not know much about what this worldsheet theory is for specific free gauge theories, but we expect that we should be able to put it into a conformal gauge, in which the space-time correlation functions are equal to correlation functions of integrated vertex operators $\int d^2z V_{\mathcal{O}}(x; z)$. In this gauge, all physical worldsheet vertex operators should have worldsheet scaling dimension $(h, \bar{h}) = (1, 1)$. In particular, we expect each single-trace gauge-invariant operator $\mathcal{O}(x) = \text{Tr}(\cdots(x))$ of the space-time theory (with or without derivatives) to correspond to a vertex operator of this dimension.

A natural object to consider in the worldsheet theory is the worldsheet OPE; we expect that as $z \rightarrow w$, the product $V_{\mathcal{O}_i}(x; z)V_{\mathcal{O}_j}(y; w)$ of two physical vertex operators should have an expansion in local worldsheet operators of the form

$$V_{\mathcal{O}_i}(x; z)V_{\mathcal{O}_j}(y; w) \sim \sum_k (z - w)^{h_k - 2} (\bar{z} - \bar{w})^{\bar{h}_k - 2} C_{ijk}(x, y) V_k(z), \quad (14)$$

where the operators V_k which appear have worldsheet scaling dimensions (h_k, \bar{h}_k) . Obviously, there is no reason why the operators on the right-hand side of (14) should all be physical operators; we expect the OPE in general to include both physical operators (of dimension $(1, 1)$, leading to an OPE coefficient proportional to $1/|z - w|^2$) and other operators with various dimensions.

As in any theory, the OPE coefficients C_{ijk} are related to the three-point functions of the operators $V_{\mathcal{O}_i} V_{\mathcal{O}_j} V_k$ (the two are proportional to each other in a basis where the two-point functions of the V_k ’s are diagonal). In particular, they should be non-vanishing whenever the three-point function is non-vanishing. Thus, if we have a non-vanishing

three-point function of three operators in space-time (as implied, for instance, by (13)), we know that the OPE coefficient of the corresponding physical worldsheet operators should also be non-vanishing. In this case, where V_k corresponds to a physical operator, the operators V_k are labeled by a space-time position u , such that the sum in (14) is really an integral, and the OPE coefficients $C_{ijk}(x, y)$ are a product of powers¹⁰ of $|x - y|$, $|x - u|$ and $|y - u|$ (we will discuss the precise form in more detail below). It is natural to expect that also the non-physical vertex operators appearing in the OPE should have a space-time interpretation, but it is not completely clear that only local space-time operators should appear. Note that in this discussion (as above) we assumed that the free field theory lives on Minkowski space; obviously for a theory living (for instance) on a compact space-time, we could expand all the gauge-invariant operators in Kaluza-Klein modes on the compact space-time and the OPE discussed above would be discrete rather than continuous.

In the previous paragraph we discussed one source of a continuum appearing in the OPE, related to the non-compactness of the Minkowski space-time which the field theory lives on. In some sense this continuum is fake, because if we label the operators by their space-time momentum p rather than their position x , defining $\tilde{V}_{\mathcal{O}_i}(p; w) = \int d^4x e^{ipx} V_{\mathcal{O}_i}(x; w)$, then the momentum of the operator appearing on the right-hand side of a product of \tilde{V} 's would be determined by momentum conservation and this continuum would disappear. However, in string theories which provide holographic descriptions of field theories there is another source of a continuum which does not disappear even in momentum space. When we have a “bulk space-time” interpretation of these string theories, for instance (for conformal field theories) as sigma models on anti-de Sitter space, this continuum arises from the non-compactness of the “radial direction” which is holographically related to the energy scale of the dual field theory. For physical vertex operators, corresponding to on-shell fields in this “bulk space-time” (but not in the original field theory), the dependence on this “radial direction” is determined by the momentum in the field theory directions; but we expect to have also unphysical vertex operators, loosely corresponding to off-shell fields in the “bulk space-time”, which can have an arbitrary dependence on the “radial direction”, leading to a continuum of operators with various worldsheet dimensions.

In general we would expect all the operators with the appropriate quantum numbers

¹⁰In general, contact terms could also appear.

to appear in the worldsheet OPE, so we would expect the right-hand side of (14) to include a continuum of dimensions (note that this is different from the continuum coming from the non-compact space-time directions for the physical vertex operators discussed above, for which all the operators had the same worldsheet dimension). The existence of such a continuum is expected on general grounds, and it explicitly appears in the worldsheet OPE whenever the worldsheet theory holographically dual to a field theory is known, for example in sigma models on AdS_3 [21, 22] or $SL(2)/U(1)$ [23]. One technical reason which necessitates the appearance of such a continuum is that the space-time theory has non-vanishing planar two-point functions (for instance $\langle \text{Tr}(\Phi^n(x)) \text{Tr}(\Phi^n(y)) \rangle$), while in standard string theories all two-point functions on the sphere vanish; this is consistent because the operators of the worldsheet theory are generally labeled by a continuous parameter j (determining their dependence on the “radial position”) such that their two-point functions behave as $V_{j_1} V_{j_2} \propto \delta(j_1 - j_2)$, and the infinity in the delta function cancels the infinity from the volume of the symmetry group of the sphere with two punctures [24]. Another reason why a continuum must always appear is that, as discussed above, physical vertex operators on the right-hand side of (14) lead to an OPE behaving as $1/|z - w|^2$. If we look at an n -point function involving the operators $V_{\mathcal{O}_i}(z)$ and $V_{\mathcal{O}_j}(w)$ with $n > 3$, the position z should be integrated over, and such a behavior would lead to a divergent integral in the region $z \sim w$ (unless the correlation function of V_k with the other operators in the correlator vanishes, which we do not expect to happen generically). On the other hand, the position space space-time correlation functions in the free field theory (assuming the operators are normal-ordered) are all finite, and we do not expect any divergences to appear. The resolution is that in general the physical vertex operator on the right-hand side would appear as part of a continuum of operators V_α of worldsheet scaling dimension $2 + \alpha$, and the correlator would behave as $\int d^2z \int d\alpha C_\alpha / |z - w|^{2-\alpha}$ rather than as $\int d^2z / |z - w|^2$; we expect that the form of C_α should be such that no divergence appears as $z \rightarrow w$, and again this is confirmed in the cases of AdS_3 and $SL(2)/U(1)$ where one can explicitly analyze the worldsheet theory.

So far we have separately discussed our expectations concerning the space-time and worldsheet OPEs; we now ask if there is any relation between them. As we mentioned above, in general there is no such relation. We expect that any operator appearing in the

space-time OPE should also appear as a physical operator in the worldsheet OPE, but in general many more operators (physical or unphysical) should also appear in the worldsheet OPE, which have no clear interpretation in the space-time OPE. However, it is still natural to expect that the worldsheet OPE should have some space-time interpretation, since when two points on the worldsheet come together, one expects their images in space-time to come together as well. Thus, we expect that the leading terms in the worldsheet OPE will depend strongly on the space-time positions x, y labeling the worldsheet operators. In some cases we expect contact terms (behaving as a derivative of a delta function of $x - y$) to appear, while in other cases, when the OPE includes a worldsheet operator which can be interpreted as a local space-time operator at a position u , we expect the coefficients to diverge as x, y and u come together. Again, these expectations are confirmed in the known case of AdS_3 , and we will see that they are also confirmed by the OPEs we will find below.

As discussed above, we expect many of the operators appearing on the right-hand side of the OPE (14) to behave as local operators in space-time (even though, when they are not physical, they do not map to actual space-time operators). Then, a specific term in the OPE takes the form

$$V_{\mathcal{O}_i}(x; z)V_{\mathcal{O}_j}(y; w) \sim \int d^d u (z - w)^{h_k - 2} (\bar{z} - \bar{w})^{\bar{h}_k - 2} C_{ijk}(x, y, u) V_k(u; z). \quad (15)$$

It is natural to expect that the operators V_k should scale under space-time scaling transformations with a fixed scaling dimension Δ_k (for example, the physical vertex operator on the worldsheet corresponding to $\text{Tr}(\Phi^n(x))$ should scale under space-time scaling transformations as an operator of dimension n). Naively we can then use the conformal symmetry to determine the space-time dependence of C_{ijk} ; for a scalar (in space-time) operator we would obtain

$$C_{ijk}(x, y, u) = C_{ijk} |x - y|^{d - \Delta_k - \Delta_i - \Delta_j} |x - u|^{\Delta_j - \Delta_i - d + \Delta_k} |y - u|^{\Delta_i - \Delta_j - d + \Delta_k}. \quad (16)$$

However, as mentioned in the previous section, the translation of [11] from the space-time to the worldsheet does not preserve the full conformal group, but just the Poincaré and scaling symmetries. These do not constrain the coefficients to the form (16), but more general forms are also allowed (of overall space-time scaling dimension $\Delta_i + \Delta_j + d - \Delta_k$). In our analysis of four-point functions below, we will see that indeed more general forms do arise which are not consistent with the full conformal symmetry group.

4 Sphere Diagrams

We begin our analysis of the worldsheet properties of the string theory dual to free gauge theories with planar (sphere) amplitudes. The analysis of general amplitudes is complicated already at this level, even for correlators with a small number of insertions, because finding the Strebel differential involves solving implicit integral equations as well as simple algebraic ones. We will show that one can learn interesting lessons by considering very simple special diagrams. We begin by discussing the simplest example, of three-point functions on the sphere, to illustrate how the general formalism works. Then, we calculate the simplest four and five-point diagrams one can construct. The analysis of more general cases (on which we were not able to make as much progress) may be found in appendix A.

4.1 Three-point function on the sphere

The simplest non-trivial correlation function in a standard string theory is the three-point function on the sphere (for string duals to field theories there are also planar two-point functions, but we will not discuss them here). In this case there is no moduli space, since we can use the worldsheet conformal symmetry to fix the three insertions on the worldsheet to $z = 0, 1, \infty$. Thus, the worldsheet three-point function is exactly the same as the space-time three-point function. However, as described above, in Gopakumar's formalism we work on the decorated moduli space, and translate the Feynman diagrams into functions on the decorated moduli space (whose integral over the circumferences p_i gives the closed string correlator). For a three-point function this decorated moduli space is three dimensional.

For simplicity, we consider only simple scalar correlation functions (in four dimensional gauge theories) of the form

$$\langle \text{Tr}(\Phi^{J_1}(x_1)) \text{Tr}(\Phi^{J_2}(x_2)) \text{Tr}(\Phi^{J_3}(x_3)) \rangle_{S^2}. \quad (17)$$

The most general Strebel differential for this problem is¹¹:

$$q = -\frac{1}{4\pi^2} \left(a \left(\frac{dz}{z} \right)^2 + b \left(\frac{dz}{1-z} \right)^2 + c \left(\frac{dz}{z(1-z)} \right)^2 \right), \quad (18)$$

¹¹The essential part of the analysis appears in [18].

where the parameters a, b, c are related to the residues p_i by

$$a = \frac{1}{2} (p_0^2 + p_\infty^2 - p_1^2), \quad b = \frac{1}{2} (p_1^2 + p_\infty^2 - p_0^2), \quad c = \frac{1}{2} (p_0^2 + p_1^2 - p_\infty^2). \quad (19)$$

This equation gives us a simple explicit formula for the Strebel differential as a function of the coordinates of the decorated moduli space. There are three different types of possible critical graphs, depending on where we are in the decorated moduli space. The three cases are characterized by the sign of $\Delta \equiv ab + ac + bc$:

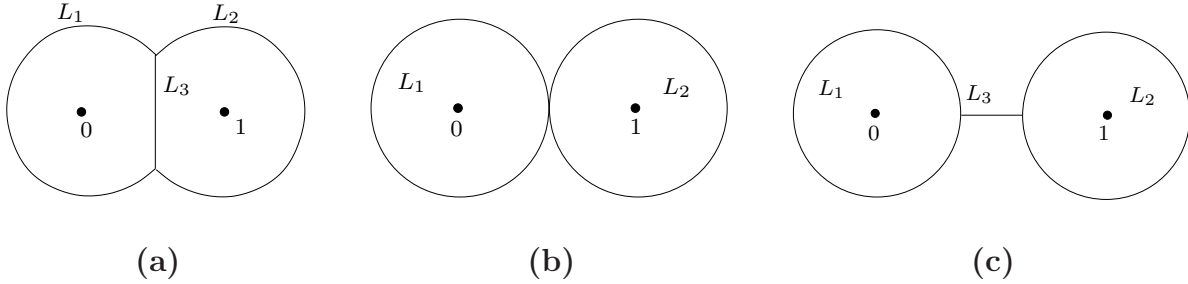


Figure 4: The three possibilities for the topology of the critical curves of the Strebel differential : **(a)** $\Delta > 0$, **(b)** $\Delta = 0$, **(c)** $\Delta < 0$.

- $\Delta > 0$: A representative critical graph for this case is drawn in Figure 4(a). The relation between the edge lengths L_i of the critical graph and the circumferences p_i is given by

$$L_1 = \frac{1}{2}(p_0 + p_\infty - p_1), \quad L_2 = \frac{1}{2}(-p_0 + p_\infty + p_1), \quad L_3 = \frac{1}{2}(p_0 - p_\infty + p_1). \quad (20)$$

The quantity Δ for this graph is equal to $16L_1L_2L_3(L_1 + L_2 + L_3)$, which is indeed positive.

- $\Delta = 0$: This is a degenerate case (see Figure 4(b) for an example) in which the two zeros of the Strebel differential have joined together, and one of the edges has degenerated; in the case depicted in the figure (the other cases are related by permutations of the points) the edge lengths are given by:

$$L_1 = p_0, \quad L_2 = p_1, \quad p_\infty = p_0 + p_1. \quad (21)$$

- $\Delta < 0$: In this case the topology of the critical graph is given by Figure 4(c) (up to permutations of the three points), and the edge lengths are given by:

$$L_1 = p_0, \quad L_2 = p_1, \quad L_3 = \frac{1}{2}(p_\infty - p_1 - p_0). \quad (22)$$

In Figure 5 we show where each of the different possible three-point critical graphs appears in the decorated moduli space.

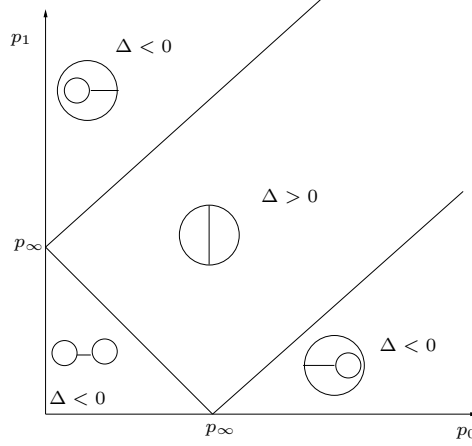


Figure 5: The critical graphs in the different regions in the decorated moduli space. We exhibit a slice with constant p_∞ . On the lines $p_0 + p_1 = p_\infty$ and $p_0 = p_1 \pm p_\infty$ we have the interpolating degenerate diagram, such as Figure 4(b).

After writing down the Strebel differentials we can translate any given three-point function in the gauge theory to the string theory language, writing it as an integral over the decorated moduli space. In each region we have a different critical graph corresponding to a different dual field theory graph, so a given Feynman diagram will contribute only in one of the three regions described above. We now discuss the translation in each of the three regions :

- $\Delta > 0$: The gauge theory diagram for this case is given in Figure 6(a) (which is the dual graph of Figure 4(a)). As a specific example, we discuss the correlation function $\langle \text{Tr}(\Phi^2(x_1)) \text{Tr}(\Phi^2(x_2)) \text{Tr}(\Phi^2(x_3)) \rangle_{S^2}$ for which this is the only contributing diagram. When written in terms of the inverse Schwinger parameters σ_i , which we

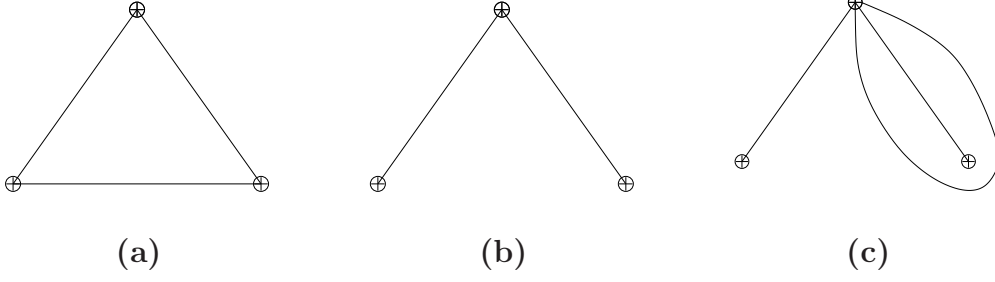


Figure 6: The possible gauge theory graphs : **(a)** $\Delta > 0$, **(b)** $\Delta = 0$, **(c)** $\Delta < 0$. In this paper we denote composite operators by a circle with a cross in it.

identify with the lengths L_i of the critical graph, the diagram is given by

$$G = A \int d\sigma_1 d\sigma_2 d\sigma_3 e^{-\frac{(x_2-x_1)^2 \sigma_1}{4}} e^{-\frac{(x_2-x_3)^2 \sigma_2}{4}} e^{-\frac{(x_3-x_1)^2 \sigma_3}{4}} = \frac{64A}{(x_2-x_1)^2 (x_3-x_1)^2 (x_2-x_3)^2}, \quad (23)$$

where A is a numerical factor. To write this expression as an integral over the circumferences we use the dictionary (20). The integral then becomes

$$G = \frac{1}{2} A \int_0^\infty dp_0 \int_0^\infty dp_1 \int_{|p_0-p_1|}^{p_0+p_1} dp_\infty e^{-\frac{p_0}{8}((x_2-x_1)^2 - (x_2-x_3)^2 + (x_3-x_1)^2)} \times e^{-\frac{p_1}{8}(-(x_2-x_1)^2 + (x_2-x_3)^2 + (x_3-x_1)^2)} e^{-\frac{p_\infty}{8}((x_2-x_1)^2 + (x_2-x_3)^2 - (x_3-x_1)^2)}, \quad (24)$$

which is our final expression for the amplitude as a function on the decorated moduli space (note that it is only non-zero in the region where $\Delta > 0$). The generalization to the contribution of this diagram to $\langle \text{Tr}(\Phi^{J_1}(x_1)) \text{Tr}(\Phi^{J_2}(x_2)) \text{Tr}(\Phi^{J_3}(x_3)) \rangle_{S^2}$ is simply given by adding appropriate powers of σ_i 's in (23).

- $\Delta = 0$: The topology of the corresponding gauge theory graph in this case is given by Figure 6(b). This graph contributes, for instance, to correlation functions of the form $\langle \text{Tr}(\Phi^{J_1}(x_1)) \text{Tr}(\Phi^{J_1+J_2}(x_2)) \text{Tr}(\Phi^{J_2}(x_3)) \rangle_{S^2}$, for which it is the only contributing graph. For example, the $\langle \text{Tr}(\Phi^2(x_1)) \text{Tr}(\Phi^4(x_2)) \text{Tr}(\Phi^2(x_3)) \rangle_{S^2}$ correlation function is given by

$$G = \tilde{A} \int d\sigma_1 d\sigma_2 \sigma_1 \sigma_2 e^{-\frac{(x_2-x_1)^2 \sigma_1}{4}} e^{-\frac{(x_2-x_3)^2 \sigma_2}{4}} = \tilde{A} \int dp_0 dp_1 p_0 p_1 e^{-\frac{(x_2-x_1)^2 p_0}{4}} e^{-\frac{(x_2-x_3)^2 p_1}{4}} = \frac{16\tilde{A}}{(x_2-x_1)^4 (x_3-x_2)^4} \quad (25)$$

for some constant \tilde{A} . Again, the generalization to more general correlation functions is straightforward. Note that the non-zero contribution of this diagram comes just from the two-dimensional subspace of the decorated moduli space with $p_\infty = p_0 + p_1$.

- $\Delta < 0$: The topology of the corresponding graph is given by Figure 6(c). It has a (topologically non-trivial) self-contraction, so when all operators are normal-ordered it vanishes. Thus, all diagrams vanish in this part of the decorated moduli space.

To summarize, when we calculate an amplitude $\langle \text{Tr}(\Phi^{J_1}(x_1)) \text{Tr}(\Phi^{J_2}(x_2)) \text{Tr}(\Phi^{J_3}(x_3)) \rangle_{S^2}$ with no self-contractions, the multiplicities m_{ij} of the edges are given by

$$m_{ij} = \frac{1}{2} \left(\sum_k J_k \right) - \sum_k |\epsilon_{ijk}| J_k. \quad (26)$$

We always get a contribution from only one region of the decorated moduli space. If one of the m_{ij} is zero we find a contribution only from $\Delta = 0$, while if all the $m_{ij} > 0$ the only contribution comes from $\Delta > 0$. In other cases the amplitude vanishes.

4.2 The Y four-point function diagram

Now that we understand how the formalism works on the simple three-point function example we turn to four-point functions. Our main interest will be in studying the worldsheet OPE. Studying this OPE using four-point functions is somewhat subtle, since in a two dimensional conformal field theory, the non-trivial dependence on the positions in four-point functions is a function only of the cross-ratio $z = (z_1 - z_2)(z_3 - z_4)/(z_1 - z_3)(z_2 - z_4)$, and the $z \rightarrow 0$ limit can be interpreted either as $z_1 \rightarrow z_2$ or as $z_3 \rightarrow z_4$. We will see that one of the interpretations will turn out to be more natural in the computation of this subsection.

Finding the Strebel differential for a general four-point diagram is a difficult task. The most general Strebel differential for a four-point amplitude, when we choose the insertions to be at $z = \pm t, 1, \infty$, has the following form [11]:

$$q = -\frac{p_\infty^2}{4\pi^2} \frac{\prod_{i=1}^4 (c_i - z)}{(1 - z)^2 (t^2 - z^2)^2} dz^2. \quad (27)$$

The sphere four-point function has a single complex modulus t , and there are four circumferences p_i . The worldsheet OPE appears in this parametrization as $t \rightarrow 0$. Recall that

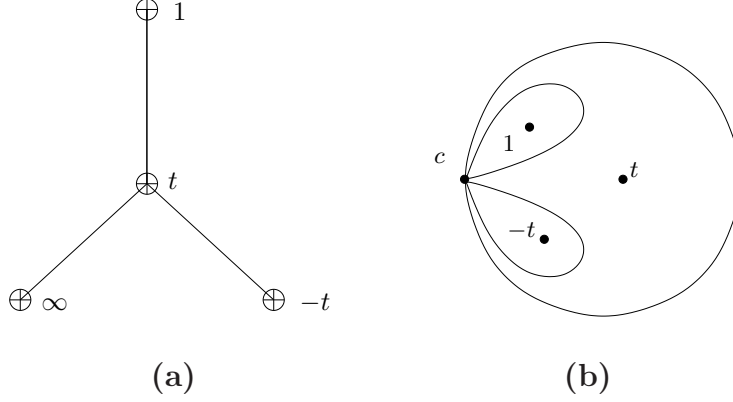


Figure 7: The Y diagram with t in the middle: **(a)** in the gauge theory, **(b)** on the worldsheet.

the field theory amplitude is given in terms of the edge lengths of the edges connecting the zeros. These are integrals of the square root of (27). The differential is Strebel when these edge lengths are real, and this gives very non-trivial equations on the parameters of (27). In the rest of this section we will consider special cases where the Strebel problem can be explicitly solved.

The first case we consider is the Y diagram of the gauge theory, drawn in Figure 7(a). We arbitrarily mapped the operator in the middle to the point t on the worldsheet, meaning that we compute the OPE between the operator in the middle and another on an edge; as discussed above, we cannot distinguish this from an OPE between the two other operators (which are both on edges) so this is in fact the most general possibility. The gauge theory scalar correlators which get contributions from this diagram are:

$$\langle \text{Tr}(\Phi^{m_t}(0)) \text{Tr}(\Phi^{m_\infty}(x_\infty)) \text{Tr}(\Phi^{m_{-t}}(x_{-t})) \text{Tr}(\Phi^{m_1}(x_1)) \rangle_{S^2} \quad (28)$$

(putting $x_t = 0$ for convenience), with $m_t = m_\infty + m_{-t} + m_1$, and this is the only diagram contributing to these correlators. The dual diagram, drawn (schematically) in Figure 7(b), consists of three disjoint disks glued at a point. Since six horizontal lines join at the vertex, it is a degenerate zero of the Strebel differential of order four. Thus, the Strebel differential for this diagram is given by:

$$q = -\frac{p_\infty^2}{4\pi^2} \left(\frac{(z-c)^2}{(z-1)(z^2-t^2)} \right)^2 dz^2. \quad (29)$$

We have three edges in this diagram, so the diagram will be non-zero only on a three real-parameter subspace of the six-real-dimensional decorated moduli space. From the figure it is clear that the four circumferences satisfy one constraint among themselves,

$$p_t = p_\infty + p_1 + p_{-t}, \quad (30)$$

so only three are independent; we can thus label the position in the subspace where the diagram is non-zero either by three of the circumferences, or by t and one of the three circumferences. In general to determine the p_i from the Strebel differential we need to take a square root of the residues p_i^2 , and there is a sign ambiguity. However, in this case (30) fixes the signs of the square roots uniquely :

$$\frac{p_t}{p_\infty} = -\frac{(c-t)^2}{2t(-t+1)}, \quad \frac{p_1}{p_\infty} = -\frac{(c-1)^2}{1-t^2}, \quad \frac{p_{-t}}{p_\infty} = -\frac{(c+t)^2}{2t(t+1)}. \quad (31)$$

Defining

$$A = \frac{p_{-t}}{p_\infty} - \frac{p_t}{p_\infty}, \quad B = \frac{p_t}{p_\infty} + \frac{p_{-t}}{p_\infty}, \quad (32)$$

we have

$$c = \frac{1}{2}(-A - tB), \quad t^2(4 + B^2 + 4A) + 2t(2B + AB) + A^2 = 0. \quad (33)$$

The discriminant of this quadratic equation with real coefficients, $\Delta = 16(B^2 - A^2)(A + 1)$, is always non-positive because of the obvious inequalities $|B| \geq |A|$ and $A \leq -1$, so the solutions for t as a function of the edge-lengths are generally complex (as expected).

Next, we would like to work out the change of variables from the Schwinger parameters (which are simply related to the edge lengths, which for this diagram are equal to p_1 , p_∞ and p_{-t}) to t and p_∞ , in order to be able to study the OPE limit $t \rightarrow 0$. The change of variables to p_∞ , A and B is straightforward. Next, we can translate A and B to t by using¹²

$$\text{Re}(t) = -\frac{2B + BA}{4 + B^2 + 4A}, \quad |t|^2 = \frac{A^2}{4 + B^2 + 4A}. \quad (34)$$

¹²It is important to emphasize that two given metric graphs of the form above which differ only in the cyclic order of the points around the graph are not in the same isomorphism class, and hence they correspond to two distinct Riemann surfaces. These two Riemann surfaces are related by complex conjugation of t .

With some algebra we find that the measure on the decorated moduli space transforms as

$$\int dp_\infty dA dB = \int dp_\infty d^2t |\text{Im}(t)| \left| \frac{4A((A+2)^2 - B^2)}{(B^2 + 4A + 4)^3} \right|^{-1}. \quad (35)$$

Next, we examine the field theory amplitude, and integrate over p_∞ . The field theory amplitude (28) in position space, when expressed in terms of the inverse Schwinger parameters, is given up to a constant by

$$G = \int dp_\infty dp_{-t} dp_1 p_\infty^{(m_\infty-1)} p_{-t}^{(m_{-t}-1)} p_1^{(m_1-1)} e^{-p_\infty(x_\infty^2 + x_{-t}^2(B+A)/2 - x_1^2(1+A))}, \quad (36)$$

which may be rewritten (after changing variables using (35) and integrating over p_∞) in the convenient form

$$G = \int d^2t |\text{Im}(t)| (x_\infty^2 + x_{-t}^2(B+A)/2 - x_1^2(1+A))^{-m_\infty - m_1 - m_{-t}} \times \left| \frac{4A((A+2)^2 - B^2)}{(B^2 + 4A + 4)^3} \right|^{-1} (A+B)^{(m_{-t}-1)} (1+A)^{(m_1-1)}. \quad (37)$$

We can now consider the OPE limit $t \rightarrow 0$. Writing $t = |t|e^{i\phi}$, we find that for small t we have

$$B = \frac{2}{(1 - \cos(\phi))|t|} + O(1), \quad A = \frac{-2}{1 - \cos(\phi)} + O(|t|). \quad (38)$$

Substituting this into (37) we find that the leading term in the OPE which contributes to this diagram is given by (up to a constant) :

$$\int d^2t |t|^{m_t - m_{-t} - 2} |\sin(\phi)| (1 + \cos(\phi))^{m_1 - 1} (1 - \cos(\phi))^{m_\infty - 1} (x_{-t}^2)^{-m_t}. \quad (39)$$

As expected, only powers of $|t|$ bigger than (-2) appear, since the integration over t must be convergent. From the form of (39) we can read off the worldsheet conformal dimensions (h, \bar{h}) of the operators appearing in the leading term: generically we find operators with

$$h + \bar{h} = m_t - m_{-t} + 2, \quad h = \frac{q}{2} \ (q \in \mathbb{Z}), \quad h, \bar{h} \geq \frac{3}{2}. \quad (40)$$

For instance, for $m_t = 7$, $m_{-t} = 2$, we have

$$(h, \bar{h}) = \left(\frac{3}{2}, \frac{11}{2}\right), (2, 5), \left(\frac{5}{2}, \frac{9}{2}\right), (3, 4), \left(\frac{7}{2}, \frac{7}{2}\right), (4, 3), \left(\frac{9}{2}, \frac{5}{2}\right), (5, 2), \left(\frac{11}{2}, \frac{3}{2}\right). \quad (41)$$

Note that, as expected, the OPE coefficient becomes singular as x_t approaches x_{-t} (this is why it is more natural to interpret this OPE in terms of these two points approaching each

other, rather than the other two points). As discussed in section 3, when the space-time theory has a conformal symmetry (as in our case), we would expect that for every value of t the worldsheet correlation function should transform under the conformal symmetry in the same way as the full space-time correlation function (given by the integral over t). However, it is easy to see that this is not the case; the ratio between the expression $(x_{-t}^2)^{-m_t}$ which we found for small t and the exact field theory answer $(x_{-t}^2)^{-m-t}(x_\infty^2)^{-m_\infty}(x_1^2)^{-m_1}$ cannot be written as a function of the two cross-ratios $(x_\infty - x_{-t})^2 x_1^2 / (x_\infty - x_1)^2 x_{-t}^2$ and $x_\infty^2 (x_{-t} - x_1)^2 / (x_\infty - x_1)^2 x_{-t}^2$, as conformal invariance would demand. However, our small t expression does have the correct scaling transformation (consistent with our discussion in section 3).

Next, we calculate the subleading term in the expansion of the OPE. The leading correction to (38) is given by

$$\begin{aligned} B &= \frac{2}{(1 - \cos(\phi))|t|} + \frac{2|t|(\cos(\phi) - \frac{1}{2})(\cos(\phi) + 1)}{\cos(\phi) - 1} + O(|t|^2), \\ A &= \frac{-2}{1 - \cos(\phi)} - \frac{|t|^2 \cos(\phi)(\cos(\phi) + 1)}{\cos(\phi) - 1} + O(|t|^3). \end{aligned} \quad (42)$$

Using (37) we find that the subleading term in the worldsheet OPE is

$$\begin{aligned} &\int d^2t |t|^{m_t - m_{-t} - 1} |\sin(\phi)| (1 + \cos(\phi))^{m_1 - 1} (1 - \cos(\phi))^{m_\infty - 1} (x_{-t}^2)^{-m_t - 1} \times \\ &\times (x_{-t}^2(1 - m_\infty - m_1) + x_\infty^2(\cos(\phi) - 1)m_t - x_1^2(\cos(\phi) + 1)m_t). \end{aligned} \quad (43)$$

The qualitative behavior is similar to that of the leading term, but now we find a different space-time dependence for different terms in the OPE (with the same $h + \bar{h}$ but different h), as we would generally expect.

Even though this diagram is quite simple, we showed that it is possible to use it to study many of the features of the gauge-string duality that we are trying to understand.

4.3 The Π four-point function diagram

The next solvable four-point function we consider is the other diagram with three edges, which we call the Π diagram (Figure 8). It contributes to various correlators in general field theories; for example, in a free gauge theory with three adjoint scalar fields Φ_1, Φ_2, Φ_3

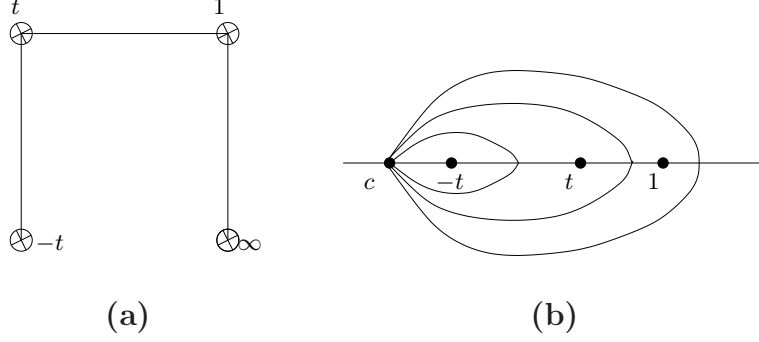


Figure 8: The Π diagram: **(a)** in the gauge theory, **(b)** on the worldsheet.

it is the only contribution to the correlator :

$$\langle \text{Tr}(\Phi_1^2(x_1)) \text{Tr}(\Phi_1^2\Phi_2(x_2)) \text{Tr}(\Phi_2\Phi_3^2(x_3)) \text{Tr}(\Phi_3^2(x_4)) \rangle_{S^2}. \quad (44)$$

We will see that this diagram has a very strange property – the string theory amplitude has support only for real values of t (namely, when all four points lie on a straight line in the plane).

The Strebel differential here is again given by:

$$q = -\frac{p_\infty^2}{4\pi^2} \left(\frac{(z-c)^2}{(z-1)(z^2-t^2)} \right)^2 dz^2, \quad (45)$$

but with a different relation between the circumferences. When we label the points as in Figure 8, we have

$$p_t - p_{-t} = p_1 - p_\infty. \quad (46)$$

The only possible sign choice is then

$$\frac{p_{\pm t}}{p_\infty} = \frac{(c \mp t)^2}{2t(\mp t + 1)}, \quad \frac{p_1}{p_\infty} = \frac{(c-1)^2}{1-t^2}. \quad (47)$$

Again, it is convenient to define

$$A = \frac{p_{-t}}{p_\infty} - \frac{p_t}{p_\infty}, \quad B = \frac{p_t}{p_\infty} + \frac{p_{-t}}{p_\infty}. \quad (48)$$

Then, we have

$$2c = A + tB, \quad (A + tB)^2 = 4t(B + tA - t). \quad (49)$$

The last equation gives t for a given value of the circumferences. We would naively expect to have solutions for all values of t near zero, in order to get an expression with a smooth OPE expansion. However, this turns out not to be the case; equation (49) gives :

$$t^2(B^2 - 4A + 4) + 2t(AB - 2B) + A^2 = 0. \quad (50)$$

This is a quadratic equation with real coefficients. The discriminant is

$$\Delta = 4(AB - 2B)^2 - 4A^2(B^2 - 4A + 4) = 16(A^2 - B^2)(A - 1). \quad (51)$$

This is always non-negative by the obvious inequalities $B \geq |A|$ and $A \leq 1$. So, these diagrams always correspond to real values of t , covering just a one-dimensional subspace of the moduli space. Thus, in this case, if we translate a correlation function such as (44) to the worldsheet, we find a non-smooth correlation function on the worldsheet which is non-zero only on a one-dimensional subspace. Obviously, this does not have a good OPE expansion, and it cannot arise from a sensible local field theory on the worldsheet. Perhaps there are some global zero modes causing this worldsheet correlation function to vanish for generic values of t .

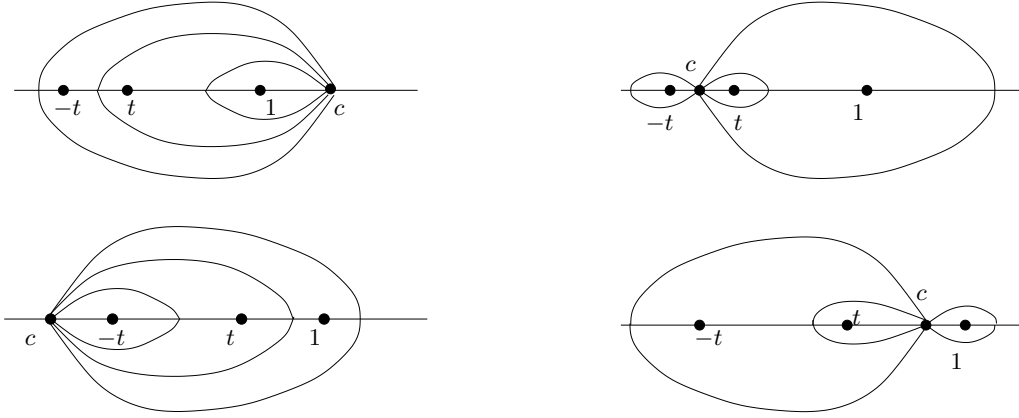


Figure 9: The four possible positions of the zero c and the structure of critical leaves implied by the symmetry of reflections round the real axis. The two critical curves on the left (and on the right) are different as metric graphs because they have a different orientation.

Note that our choice (46) by itself does not uniquely determine the topology of the critical curve; there are four topologically distinct critical curves obeying this relation. We

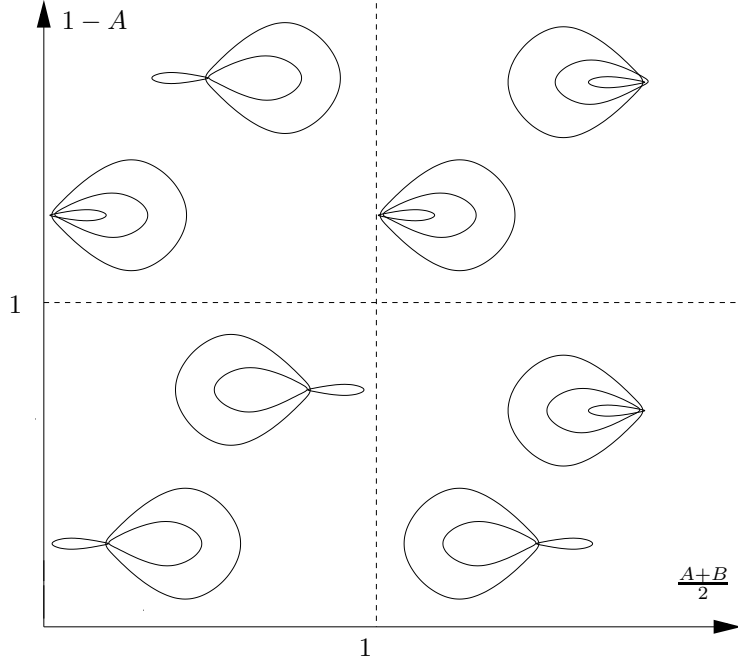


Figure 10: The four regions of A, B space; for each A, B there are two possible solutions of the quadratic equation, and we draw the two distinct diagrams that they corresponds to. As explained, each metric graph (including orientation) appears exactly once.

draw these four possibilities in Figure 9. The differential in this case is real, so the critical lines are obviously invariant under reflection with respect to the real axis. At first sight one may worry that we obtain from the quadratic equation (50) above two different solutions for t with the same circumferences, even though the Strebel isomorphism should give a unique (marked) Riemann surface for every value of the edge lengths. The resolution is that the two solutions have different topologies, so they correspond to different graphs (Feynman diagrams) on the field theory side. The summary of the possible graphs which appear for each value of the circumferences (labeled by A and B) is given in Figure 10.

4.4 The X five-point function diagram

The final example we discuss in detail is the five-point X amplitude, drawn in Figure 11. This is the single contribution to correlators of the form

$$\langle \text{Tr}(\Phi^{m_1}(x_1)) \text{Tr}(\Phi^{m_b}(x_b)) \text{Tr}(\Phi^{m_\infty}(x_\infty)) \text{Tr}(\Phi^{m_{-t}}(x_{-t})) \text{Tr}(\Phi^{m_t}(x_t)) \rangle_{S^2}, \quad (52)$$

with $m_t = m_1 + m_b + m_\infty + m_{-t}$. Here we will illustrate how the fact that the string theory amplitude localizes on a sub-manifold of the moduli space makes it difficult to extract the OPE.

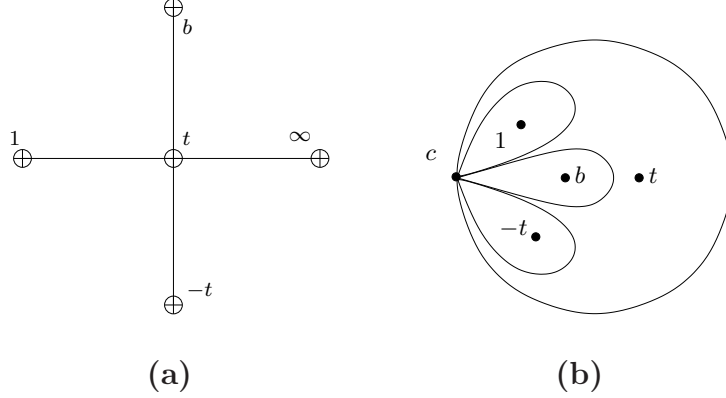


Figure 11: The X diagram: **(a)** in the gauge theory, **(b)** on the worldsheet.

The Strebel differential in this case has a zero of order six, so it is given by (choosing the insertions at $z = 1, \pm t, b, \infty$):

$$q = -\frac{p_\infty^2}{4\pi^2} \frac{(c-z)^6}{(1-z)^2(b-z)^2(t^2-z^2)^2} dz^2. \quad (53)$$

The ratios of the circumferences are given by (denoting $p_t = p_+$, $p_{-t} = p_-$)

$$\begin{aligned} \frac{p_1}{p_\infty} &= \gamma_1 \frac{(c-1)^3}{(1-t^2)(b-1)} \equiv \alpha_1^3, & \frac{p_b}{p_\infty} &= \gamma_b \frac{(c-b)^3}{(b^2-t^2)(b-1)} \equiv \alpha_b^3, \\ \frac{p_+}{p_\infty} &= \gamma_+ \frac{(c-t)^3}{2t(1-t)(b-t)} \equiv \alpha_+^3, & \frac{p_-}{p_\infty} &= \gamma_- \frac{(c+t)^3}{2t(1+t)(b+t)} \equiv \alpha_-^3, \end{aligned} \quad (54)$$

up to signs γ_i , which depend on the choice of which vertex we put in the middle; note the useful identity

$$\frac{(c-1)^3}{(1-t^2)(b-1)} - \frac{(c-b)^3}{(b^2-t^2)(b-1)} - \frac{(c-t)^3}{2t(1-t)(b-t)} + \frac{(c+t)^3}{2t(1+t)(b+t)} - 1 = 0. \quad (55)$$

If we put the vertex at the point j in the middle we have:

$$\sum_{i \neq j} \frac{p_i}{p_j} - 1 = 0. \quad (56)$$

There are two possible cases to consider when taking the small t limit : either putting one of $\pm t$ in the middle, or putting both on the edges.

On the field theory side we have four edge-length parameters, which should map to a subspace of the decorated moduli space (the circumferences, b and t). As discussed in section 2 we have a $p_i \rightarrow \alpha p_i$ scaling symmetry which does not change the Riemann surface (and rescales the edge lengths), so we will cover at most a three real-dimensional subspace of the moduli space (the space of b 's and t 's).

As in the previous examples, we can solve the equations above to get all the constraints, without any need to invoke the reality conditions of the Strebel differential (which are automatically satisfied). We define

$$F_1 = \gamma_1^{1/3} \left((1 - t^2)(b - 1) \right)^{1/3}, \quad F_{\pm} = \gamma_{\pm}^{1/3} \left(2t(1 \mp t)(b \mp t) \right)^{1/3}, \quad (57)$$

where we choose a specific root for the third root of the expressions in the brackets, and the ambiguity is swallowed in the third root of the γ 's. The equations for the circumferences become:

$$\alpha_1 F_1 + 1 = c, \quad \alpha_+ F_+ + t = c, \quad \alpha_- F_- - t = c. \quad (58)$$

We take all the α_i to be real and positive. The first equation can be taken to be an equation for c , and from the two others we get four real equations. Two are equations for α_{\pm} :

$$2t_1 = \alpha_- \text{Re}(F_-) - \alpha_+ \text{Re}(F_+), \quad 2t_2 = \alpha_- \text{Im}(F_-) - \alpha_+ \text{Im}(F_+), \quad (59)$$

where $t_1 \equiv \text{Re}(t)$ and $t_2 \equiv \text{Im}(t)$. One equation gives α_1 ,

$$\alpha_1 = \text{Re} \left(\frac{t + \alpha_+ F_+ - 1}{F_1} \right), \quad (60)$$

and the last one is a constraint on the moduli space:

$$0 = \text{Im} \left(\frac{t + \alpha_+ F_+ - 1}{F_1} \right). \quad (61)$$

The equations for α_{\pm} are easily solved:

$$\alpha_{\pm} = 2 \frac{t_2 \text{Re}(F_{\mp}) - t_1 \text{Im}(F_{\mp})}{\text{Re}(F_+) \text{Im}(F_-) - \text{Re}(F_-) \text{Im}(F_+)}. \quad (62)$$

We begin with the case when the two $\pm t$ insertions are on the edges. Without loss of generality we take ∞ to be in the middle. For this choice the signs are

$$\gamma_1 = -\gamma_b = -\gamma_+ = \gamma_- = 1. \quad (63)$$

To the leading order in t we then get :

$$F_{\pm} = (2|tb|)^{1/3} e^{\frac{i}{3}(\pi k_{\pm} + \phi + \theta_b)}, \quad (64)$$

where k_+ is an odd integer and k_- is even, ϕ is the phase of t , and θ_b is the phase of b .

From here we find

$$\begin{aligned} \Delta &\equiv \text{Re}(F_+) \text{Im}(F_-) - \text{Re}(F_-) \text{Im}(F_+) = \\ &= (2|tb|)^{2/3} \left(\cos\left(\frac{\pi k_+ + \phi + \theta_b}{3}\right) \sin\left(\frac{\pi k_- + \phi + \theta_b}{3}\right) - \sin\left(\frac{\pi k_+ + \phi + \theta_b}{3}\right) \cos\left(\frac{\pi k_- + \phi + \theta_b}{3}\right) \right) \\ &= (2|tb|)^{2/3} \sin\left(\frac{\pi(k_- - k_+)}{3}\right). \end{aligned} \quad (65)$$

Note that if $k_- - k_+ = 3m$ we get a contradiction : we find that p_{\pm} should go as $\pm B/|t|$ for small t , which contradicts the positivity of the circumferences (because the zero c goes to a constant as $t \rightarrow 0$ if $k_- - k_+ = 3m$). Thus, the α_{\pm} are:

$$\begin{aligned} \alpha_{\pm} &= \frac{2(2|t|)^{2/3}}{|b|^{1/3} \sin\left(\frac{\pi(k_- - k_+)}{3}\right)} \left(\sin(\phi) \cos\left(\frac{\pi k_{\mp} + \phi + \theta_b}{3}\right) - \cos(\phi) \sin\left(\frac{\pi k_{\mp} + \phi + \theta_b}{3}\right) \right) \\ &= 2(2|t|)^{2/3} \frac{\sin\left(\frac{1}{3}(2\phi - \pi k_{\mp} - \theta_b)\right)}{|b|^{1/3} \sin\left(\frac{\pi(k_- - k_+)}{3}\right)}. \end{aligned} \quad (66)$$

The circumferences are:

$$\frac{p_{\pm}}{p_{\infty}} = \frac{8(2|t|)^2}{|b|} \left(\frac{\sin\left(\frac{2\phi - \pi k_{\mp} - \theta_b}{3}\right)}{\sin\left(\frac{\pi(k_- - k_+)}{3}\right)} \right)^3. \quad (67)$$

The phases k_{\pm} are set unambiguously by demanding the positivity of these expressions.

The phase choices are:

$$\begin{aligned} \phi - \frac{\theta_b}{2} \in (0, \pi) &\rightarrow (k_-, k_+) = (0, 5), (2, 3); \\ \phi - \frac{\theta_b}{2} \in (\pi, 2\pi) &\rightarrow (k_-, k_+) = (4, 5), (2, 1). \end{aligned} \quad (68)$$

There are four choices of the phases which give exactly the same results. The different choices are simply switching p_+ and p_- (relabeling the edges). We note that here $c \rightarrow 0$

as $t \rightarrow 0$, and thus $b = -p_b/p_1 \leq 0$. Thus, b is real and negative. The Jacobian for the change of variables from $p_+/p_\infty, p_-/p_\infty$ to $|t|, \phi$ is easily obtained from here : for small $|t|$

$$\mathcal{J} \sim |t|^3 \frac{\sin\left(\frac{1}{3}(2\phi - \pi k_+)\right)^2 \sin\left(\frac{1}{3}(2\phi - \pi k_-)\right)^2}{\sin\left(\frac{\pi(k_- - k_+)}{3}\right)^5}. \quad (69)$$

Note also that the constraint (61) on the moduli space reads

$$0 = \text{Im}\left[\frac{1}{F_1}\right] \rightarrow \text{Im}\left[\gamma_1^{1/3}(1 - b)\right] = 0, \quad (70)$$

so we get that $\gamma_1^{1/3} = 1$. We also have two positivity constraints for p_1, p_b which give

$$-1 \leq \text{Re}\left[\frac{1}{F_1}\right] \leq 0 \rightarrow -1 \leq \frac{1}{(b-1)^{1/3}} \leq 0, \quad (71)$$

which is satisfied. Thus all the phases are set.

Let us now discuss the case of one $\pm t$ insertion in the middle, say t . We obtain:

$$F_\pm = e^{\frac{\pi i}{3}k_\pm} (2tb)^{1/3} (1 \mp (1 + b^{-1})\frac{1}{3}t). \quad (72)$$

In this case

$$\gamma_1 = -\gamma_b = \gamma_t = \gamma_{-t} = -1. \quad (73)$$

Note that if $k_+ \neq k_-$ the equations are essentially the same as above. Thus, the p_\pm circumferences go to zero as t goes to zero. This, however, implies that the other circumferences cannot all be positive because we have $p_+ = p_- + p_1 + p_b + p_\infty$. Thus, this case is inconsistent and we must have here $k_\pm = k$ where k is odd or even depending on which insertion, $\pm t$, we chose to put in the middle. Thus we find (at leading order in $|t|$)

$$\alpha_\pm = \frac{3}{(2|tb|)^{1/3}} \left(\frac{\sin\left(\frac{1}{3}(2\phi - \pi k - \theta_b)\right)}{|1 + b^{-1}| \sin(\phi + \tilde{\theta}_b)} \pm \frac{|1 + b^{-1}| \sin\left(\frac{1}{3}(\phi + \pi k) + \theta_b + \tilde{\theta}_b\right)}{\sin(\phi + \tilde{\theta}_b)} |t| \right), \quad (74)$$

where $\tilde{\theta}_b$ is the phase of $(1 + b^{-1})$ and θ_b is the phase of b . The circumferences behave as:

$$\frac{p_\pm}{p_\infty} = \frac{27}{2|tb|} \left(\frac{\sin\left(\frac{1}{3}(2\phi - \pi k - \theta_b)\right)}{|1 + b^{-1}| \sin(\phi + \tilde{\theta}_b)} \right)^3 \left(1 \pm 3|1 + b^{-1}|^2 \frac{\sin\left(\frac{1}{3}(\phi + \pi k) + \theta_b + \tilde{\theta}_b\right)}{\sin\left(\frac{1}{3}(2\phi - \pi k - \theta_b)\right)} |t| \right). \quad (75)$$

Note that k should be chosen such that the expression will be positive, and it depends on $\tilde{\theta}_b$. The details are similar to the previous case but the expressions are more complicated so we omit them here. There is only one choice of k such that the solution is well-behaved as a function of ϕ . Also note that here α_1 depends on the phase ϕ . The Jacobian is a complicated function of the phases, because even the leading term of α_1 has a non-trivial dependence on ϕ , and b is also a complicated function of ϕ . At leading order as $t \rightarrow 0$ we find

$$\mathcal{J} = J_0(\theta_b, |b|, \phi) \frac{1}{|t|^2}, \quad (76)$$

where the Jacobian is from the integration over p_i/p_∞ to the integration over $d^2 b d|t| d\phi$.

We now calculate the string theory amplitude from the gauge theory expression as usual, for the correlation function (52). In the gauge theory we have (up to a constant)

$$\begin{aligned} G &= \int \prod_{i=-t, b, 1, \infty} d\sigma_i \sigma_i^{m_i-1} e^{-\frac{(x_i - x_t)^2}{4} \sigma_i} \\ &= \int \prod_{i=-t, b, 1} d\frac{p_i}{p_\infty} \left(\frac{p_i}{p_\infty}\right)^{m_i-1} \int dp_\infty p_\infty^{\sum_{i=-t, b, 1, \infty} (m_i-1)+3} e^{-p_\infty A} \\ &\propto \int \prod_{i=-t, b, 1} d\frac{p_i}{p_\infty} \left(\frac{p_i}{p_\infty}\right)^{m_i-1} \left(\frac{1}{A}\right)^{m_t}, \end{aligned} \quad (77)$$

where

$$A \equiv \sum_{i=-t, b, 1, \infty} \frac{(x_i - x_t)^2}{4} \frac{p_i}{p_\infty}. \quad (78)$$

We find that in the $t \rightarrow 0$ limit the amplitude has the simple form :

$$\begin{aligned} G &\propto \int d^2 t \frac{1}{(x_t - x_{-t})^{2m_t}} |t|^{m_1+m_b+m_\infty-2} \tilde{F}(\phi) \\ &= \int d^2 t \frac{1}{(x_t - x_{-t})^{2m_t}} |t|^{m_t-m_{-t}-2} \tilde{F}(\phi). \end{aligned} \quad (79)$$

The dependence on the phases here is quite complicated. The leading divergent power in the OPE agrees with what we found for the 4-point Y amplitude (39). Note that, unlike what we found before, the dependence on the phase ϕ is not a finite sum of sin's. The easy way to see this is to note that the only dependence on m_∞ in (77) comes from the term

$$\left(\frac{1}{A}\right)^{m_\infty} \sim \left(\frac{1}{(x_t - x_{-t})^2 \frac{p_{-t}}{p_\infty}}\right)^{m_\infty} \quad (80)$$

in the integrand. From the calculation of $\frac{p_{-t}}{p_{\infty}}$ above we know that the phase dependence of this term is of the form

$$\left(\frac{\sin(\phi + \tilde{\theta}_b)}{\sin\left(\frac{1}{3}(2\phi - \pi k - \theta_b)\right)} \right)^{3m_{\infty}}. \quad (81)$$

This expression does not factorize as a finite sum of trigonometric functions. However, it turns out that this is a meaningless statement because we have the delta function constraint (61) (recall that the integral is only over a three-dimensional subspace of the space of b 's and t 's), which is a functional relation among ϕ , θ_b and $|b|$ (to the leading order in $|t|$), and thus, we can substitute anything which equals one on the constraint space into the integrand. The result is that the ϕ dependence is not well defined here. On the other hand, the power of $|t|$ appearing in the OPE is well-defined, because the delta function for small $|t|$ is independent of $|t|$. This is not trivial; if the constraint had looked like (for small $|t|$) $\delta(\frac{\dots}{|t|})$, then the power of $|t|$ in the most singular term would have also been an ill-defined quantity.

An interesting point to note is that for the previous case, with the $\pm t$ insertions on the edges, the series begins with more regular terms than in the other OPEs we analyzed so far. We find that the most singular term in this case is given by :

$$G \sim \int d^2t |t|^{2(m_t + m_{-t}) - 2} \tilde{F}_2(\phi, x_i). \quad (82)$$

Our interpretation of this is that the leading terms in the OPE, going as $|t|^{|m_t - m_{-t}| - 2}$ and higher powers, do not contribute to the correlation function in this case, and the terms which contribute start at the order appearing in (82).

It is easy to generalize the procedure of this subsection to general *star* diagrams, with one point in the middle connected to $n - 1$ other points by edges. For an n -point *star* diagram, if we put $\pm t$ on the edges, we find

$$\frac{p_{\pm}}{p_{\infty}} \sim |t|^{n-3}, \quad \mathcal{J} \sim |t|^{2(n-4)}, \quad (83)$$

and we will get even higher powers of $|t|$ as the first terms of the OPE expansion. It is still true, however, that the power will depend only on the combination $m_t + m_{-t}$. On the

other hand, if we put t in the middle and $-t$ on the edge, we reproduce the same $|t|$ power that we found (for $n = 4, 5$) in the Y and X diagrams. We find here:

$$\frac{p_{\pm}}{p_{\infty}} \sim \frac{1}{|t|}, \quad \mathcal{J} \sim |t|^{-2}, \quad (84)$$

leading to a leading power of t in the OPE equal to $m_t - m_{-t} - 2$.

5 Two-Point Function on the Torus

In this section we will discuss some aspects of the two-point function on the torus (note that while in a general string theory one could have also non-zero one-point functions on the torus, these are not present in free gauge theories with normal-ordered operators so we ignore them here). In string theory, a general two-point function on a torus has four real parameters, the complex position b of one of the insertions (when the other insertion is chosen at $z = 0$) and the complex torus modulus τ . In the decorated moduli space there are two additional moduli, the two circumferences related to the two insertions. Thus, we have six real parameters for a two-point function on the torus.

If we map a generic point on this decorated moduli space to a field theory two-point function using the general prescription described in section 2, we find a toroidal Feynman diagram with six edges, but with two (topologically non-trivial) self-contractions. A toroidal 2-point function with no self-contractions has only four edges in its “skeleton graph” (see, for instance, [25] for discussions of toroidal 2-point functions in free gauge theories); thus, the non-vanishing Feynman diagrams in our theory map to a four real-dimensional subspace of the decorated moduli space. Moreover, since this subspace is clearly invariant under a rescaling of the circumferences $p_i \rightarrow \alpha p_i$ (which corresponds to a rescaling of all the Schwinger parameters, as mentioned in section 2), its projection onto the moduli space is at most a three real-dimensional space (out of the four real dimensions). So, again we find that the worldsheet correlation function vanishes at generic points on the moduli space. In this section we will investigate in detail the subspace on which the correlation function is non-vanishing. Some basic definitions and facts about elliptic functions which will be used extensively in the following may be found in Appendix B.

The non-zero toroidal two-point functions in a free field theory take the form

$$\langle \text{Tr}(\Phi^n(x_1)) \text{Tr}(\Phi^n(x_2)) \rangle_{T^2}. \quad (85)$$

We are interested in diagrams without self-contractions. It is easy to convince oneself that for such diagrams the two circumferences, p_0 and p_b , must be equal, as depicted in Figure 12(a). Any critical curve which is not topologically of the form drawn in Figure 12(a) will have self-contractions.

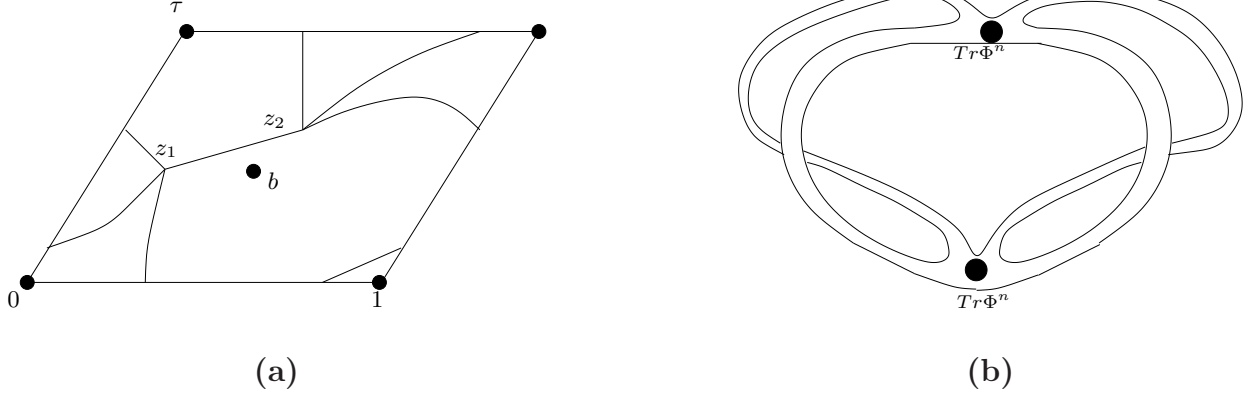


Figure 12: Two-point function on the torus without self-contractions: **(a)** The critical graph (dual to the gauge theory graph). **(b)** The gauge theory graph.

From the figure it is clear that the Strebel differential corresponding to such a graph should have two double zeros (the general two-point function on the torus will have four simple zeros, but also self-contractions). The Strebel differential should respect the periodicities of the torus and thus should be an elliptic function. For any elliptic function, the sum of the poles (weighted by their order) minus the sum of the zeros (weighted by their order) is a period of the torus. Denoting the zeros by z_i ($i = 1, 2$), this gives:

$$0 + 2b - \sum_{i=1}^4 (\text{zeros}) = 2b - 2(z_1 + z_2) = n\tau + m \quad (n, m \in \mathbb{Z}). \quad (86)$$

There are now two distinct cases, one when the zeros and poles satisfy

$$b - z_1 - z_2 = \tilde{n}\tau + \tilde{m}, \quad (\tilde{n}, \tilde{m} \in \mathbb{Z}) \quad (87)$$

and the other where

$$b - z_1 - z_2 \neq \tilde{n}\tau + \tilde{m}, \quad (\tilde{n}, \tilde{m} \in \mathbb{Z}). \quad (88)$$

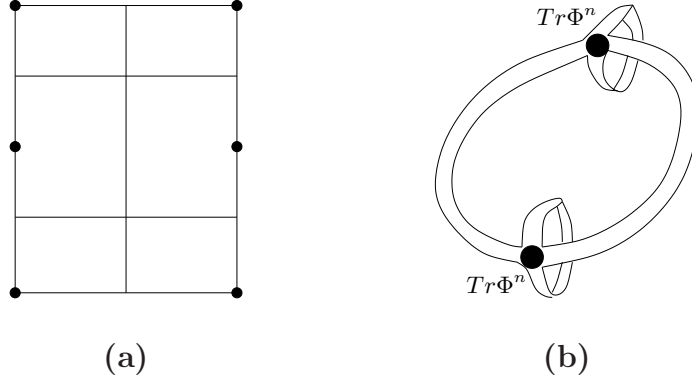


Figure 13: A specific two-point function on the torus with self-contractions, with $\tau = 2i$ and $b = i$: **(a)** Critical (dual) graph. **(b)** Gauge theory graph.

Note that our demand that the differential will have two double zeros is still not enough to rule out self-contractions. For instance, the following differential (on a torus with $\tau = 2i$) has both double zeros and self-contractions, as depicted in Figure 13:

$$q = -\frac{L^2}{4\pi^2} \wp(z \mid \tau = i) dz^2. \quad (89)$$

Note that for this differential (which has $b = i$) we are in the case (88). In the rest of this section we will analyze the general differential with no self-contractions, and we will see that it satisfies (87). Thus, we claim that any diagram with self-contractions satisfies (88), and the ones without self-contractions satisfy (87).

First, let us discuss a specific explicit example. We argue that

$$q = -\frac{L^2}{4\pi^2} \left\{ \wp(z) + \wp\left(z - \frac{\tau + 1}{2}\right) - e_1 - e_3 \right\} dz^2 \quad (90)$$

is a good Strebel differential without self-contractions for some class of τ 's. This differential has double zeros at $z = \tau/2$ and $z = 1/2$, and double poles at $z = 0$ and $z = (\tau + 1)/2$. Thus, the zeros and poles satisfy (87). We can check if this is a Strebel differential by noting that

$$q = \left(\frac{iLd\wp}{4\pi(\wp - e_2)} \right)^2, \quad (91)$$

so we can easily compute the edge lengths, say between the zeros $w_1 = 1/2$ and $w_3 = \tau/2$:

$$\sigma = \int_{w_1}^{w_3} \sqrt{q} = \frac{iL}{4\pi} \int_{e_1}^{e_3} \frac{d\wp}{\wp - e_2} = \frac{iL}{4\pi} \ln \frac{e_3 - e_2}{e_1 - e_2}. \quad (92)$$

For this to be real (note that this is independent of the branch of the log) we should have

$$\frac{e_3 - e_2}{e_1 - e_2} = e^{i\theta} \quad (93)$$

for real θ , which implies a condition on τ . This condition can be understood graphically : $e_3 - e_2$ and $e_1 - e_2$ should lie on the same circle in the \wp plane (see Figure 14). When this

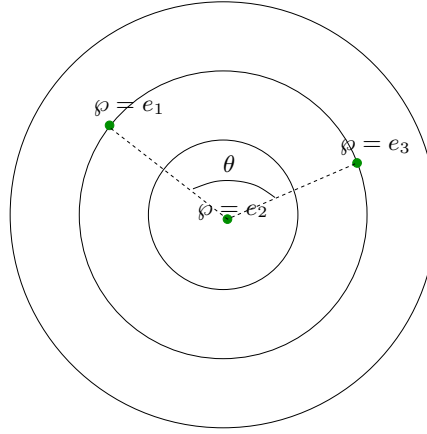


Figure 14: The \wp -plane horizontal curves of (90).

is satisfied, there will be two different edges of the critical graph with lengths:

$$\sigma_1 = L \frac{\theta(\tau)}{4\pi}, \quad \sigma_2 = L \frac{2\pi - \theta(\tau)}{4\pi}. \quad (94)$$

We note that the quantity $\frac{e_3 - e_2}{e_1 - e_2}$ is used in the mathematical literature, and is usually denoted by¹³ $k^2(\tau)$. It satisfies that for any complex $a \neq 0, 1$ there is a τ such that $k^2(\tau) = a$. Thus, the solutions to (93) give a one-dimensional subspace of the three-dimensional submanifold we are looking for. One can show that the solution of (93) is simply (in the fundamental domain) $|\tau| = 1$ ¹⁴. We will see some examples of such solutions in numerical calculations below. For these τ 's, the differential (90) is a perfectly good

¹³It satisfies $k^2(\tau) = \theta_{10}^4(0|\tau)/\theta_{00}^4(0|\tau)$.

¹⁴This can be proven using elementary modular properties of the so-called λ functions.

Strebel differential, so we have found a class of examples of differentials without self-contractions satisfying (87).

In the rest of this section we look for the most general Strebel differential which has double zeros and satisfies (87). It can be written as:

$$q = -\frac{c^2}{4\pi^2} \left(\frac{\wp(z - \frac{z_1+z_2}{2}) - \wp(\frac{z_1-z_2}{2})}{\wp(z - \frac{z_1+z_2}{2}) - \wp(\frac{z_1+z_2}{2})} \right)^2 dz^2, \quad (95)$$

which has poles of second order at 0 , $b = z_1 + z_2$ and zeros of second order at z_1 , z_2 . The equal residues are given by

$$p_0^2 = p_b^2 = c^2 \left(\frac{\wp(\frac{z_1+z_2}{2}) - \wp(\frac{z_1-z_2}{2})}{\frac{\partial \wp}{\partial z}(\frac{z_1+z_2}{2})} \right)^2. \quad (96)$$

We fix the value of τ , and we wish to find c and the zeros such that (95) is a Strebel differential with a pole at $b = z_1 + z_2$. We have solutions only for a three-dimensional submanifold of τ , b , determined by the reality of the integrals of \sqrt{q} along curves γ_i between the zeros :

$$\begin{aligned} \sigma_i &= \frac{ic}{2\pi} \int_{\gamma_i} dz \frac{\wp(z - \frac{z_1+z_2}{2}) - \wp(\frac{z_1-z_2}{2})}{\wp(z - \frac{z_1+z_2}{2}) - \wp(\frac{z_1+z_2}{2})} = \frac{ic}{2\pi} \int_{\gamma_i} dz \left(1 + \frac{\wp(\frac{z_1+z_2}{2}) - \wp(\frac{z_1-z_2}{2})}{\wp(z - \frac{z_1+z_2}{2}) - \wp(\frac{z_1+z_2}{2})} \right) = \\ &= \frac{ic}{2\pi} \left(\gamma_i(1) - \gamma_i(0) + (\wp(\frac{z_1+z_2}{2}) - \wp(\frac{z_1-z_2}{2})) \int_{\gamma_i} dz \frac{1}{\wp(z - \frac{z_1+z_2}{2}) - \wp(\frac{z_1+z_2}{2})} \right). \end{aligned} \quad (97)$$

This integral is expressible in terms of different Weierstrass functions

$$\int dz \frac{1}{\wp(z - a) - \wp(a)} = \frac{\ln \frac{\sigma(z-2a)}{\sigma(z)} + 2z\zeta(a)}{\wp'(a)}, \quad (98)$$

whose definitions are summarized in Appendix B. Denoting $\Delta z = z_2 - z_1$, we find that the three independent length-integrals lead to the equations :

- Direct $z_1 \rightarrow z_2$ integral :

$$\begin{aligned} 0 &= \text{Re} \left\{ \frac{c}{2\pi} \left(\Delta z + \frac{\wp(\frac{z_1+z_2}{2}) - \wp(\frac{\Delta z}{2})}{\wp'(\frac{z_1+z_2}{2})} \left(\ln \frac{\sigma(-z_1)}{\sigma(z_2)} - \ln \frac{\sigma(-z_2)}{\sigma(z_1)} + 2\Delta z \zeta(\frac{z_1+z_2}{2}) \right) \right) \right\} = \\ &= p_0 \text{Re} \left\{ \frac{\wp'(\frac{z_1+z_2}{2}) \Delta z}{\wp(\frac{z_1+z_2}{2}) - \wp(\frac{\Delta z}{2})} + 2\Delta z \zeta(\frac{z_1+z_2}{2}) + 2 \ln \frac{\sigma(z_1)}{\sigma(z_2)} \right\}, \end{aligned} \quad (99)$$

- $z_1 \rightarrow z_2 + 1$ integral minus $z_1 \rightarrow z_2$ integral :

$$\begin{aligned} 0 &= p_0 \operatorname{Re} \left\{ \frac{\wp'(\frac{z_1+z_2}{2})}{\wp(\frac{z_1+z_2}{2}) - \wp(\frac{\Delta z}{2})} + 2\zeta(\frac{z_1+z_2}{2}) + \ln \frac{\sigma(-z_1+1)}{\sigma(z_2+1)} - \ln \frac{\sigma(-z_1)}{\sigma(z_2)} \right\} = \\ &= p_0 \operatorname{Re} \left\{ \frac{\wp'(\frac{z_1+z_2}{2})}{\wp(\frac{z_1+z_2}{2}) - \wp(\frac{\Delta z}{2})} + 2\zeta(\frac{z_1+z_2}{2}) - 2(z_1+z_2)\eta_1 \right\}, \end{aligned} \quad (100)$$

- $z_2 \rightarrow z_1 + \tau$ integral minus $z_2 \rightarrow z_1$ integral :

$$\begin{aligned} 0 &= p_0 \operatorname{Re} \left\{ \frac{\wp'(\frac{z_1+z_2}{2})\tau}{\wp(\frac{z_1+z_2}{2}) - \wp(\frac{\Delta z}{2})} + 2\tau\zeta(\frac{z_1+z_2}{2}) - 2(z_1+z_2)\eta_3 \right\} = \\ &= p_0 \operatorname{Re} \left\{ \frac{\wp'(\frac{z_1+z_2}{2})\tau}{\wp(\frac{z_1+z_2}{2}) - \wp(\frac{\Delta z}{2})} + 2\tau\zeta(\frac{z_1+z_2}{2}) - 2(z_1+z_2)\tau\eta_1 + 2i(z_1+z_2)\pi \right\} \end{aligned} \quad (101)$$

It is possible to combine the last two equations into

$$\frac{\wp'(\frac{z_1+z_2}{2})}{\wp(\frac{z_1+z_2}{2}) - \wp(\frac{\Delta z}{2})} + 2\zeta(\frac{z_1+z_2}{2}) - 2(z_1+z_2)\eta_1 = -2i\pi \operatorname{Im}(z_1+z_2)/\tau_2, \quad (102)$$

which is further conveniently rewritten as

$$\wp(\frac{\Delta z}{2}) = \frac{\wp'(\frac{z_1+z_2}{2})}{2\zeta(\frac{z_1+z_2}{2}) - 2(z_1+z_2)\eta_1 + 2i\pi \operatorname{Im}(z_1+z_2)/\tau_2} + \wp(\frac{z_1+z_2}{2}). \quad (103)$$

An immediate consequence is that for small $b = z_1 + z_2$ we have

$$\wp(\frac{\Delta z}{2}) \sim \left(-2\eta_1 + \frac{2\pi i \operatorname{Im}(b)}{\tau_2} \right) + O(b) = O(1), \quad (104)$$

which means that both of the zeros approach a constant (depending on the phase of b) as $b \rightarrow 0$.

We define a function $K(z_{1,2}, \bar{z}_{1,2}, \tau, \bar{\tau})$ by the inverse Weierstrass function acting on (103) :

$$\frac{\Delta z}{2} = \wp^{-1} \left(\frac{\wp'(\frac{z_1+z_2}{2})}{2\zeta(\frac{z_1+z_2}{2}) - 2(z_1+z_2)\eta_1 + 2i\pi \operatorname{Im}(z_1+z_2)/\tau_2} + \wp(\frac{z_1+z_2}{2}) \right) \equiv K(z_{1,2}, \bar{z}_{1,2}, \tau, \bar{\tau}). \quad (105)$$

Plugging this result back into (99) we get an equation directly for $z_{1,2}$ so that the differential (95) is a Strebel differential on the torus with modulus τ and with a marked point at $(z_1 + z_2) \bmod(\text{lattice})$:

$$0 = \operatorname{Re} \left\{ \left(2(z_1+z_2)\eta_1 - \frac{2i\pi \operatorname{Im}(z_1+z_2)}{\tau_2} \right) K(z_{1,2}, \bar{z}_{1,2}, \tau, \bar{\tau}) + \ln \frac{\sigma(\frac{z_1+z_2}{2} - K(z_{1,2}, \bar{z}_{1,2}, \tau, \bar{\tau}))}{\sigma(\frac{z_1+z_2}{2} + K(z_{1,2}, \bar{z}_{1,2}, \tau, \bar{\tau}))} \right\}. \quad (106)$$

Note that, as expected, the definition of K and equation (106) depend only on $z_1 + z_2$, so this gives a real equation for b and τ ; however, we chose to write the equation as an equation for the z_i and not for b because it is periodic under simultaneous shifts of z_1 and z_2 by $n + m\tau$, but not under general lattice shifts of $z_1 + z_2$ (although the space of solutions for $b = z_1 + z_2$ is of course periodic). In practice, we solve for the sum of the zeros and then b is uniquely determined, modulo the lattice. We are now able to find directly the curves on which b can lie. We expect that for a generic τ the insertion b can be moved on some curves in the fundamental domain. In Figure 15 we show these curves (computed numerically from (106)) for some representative values of τ . For some special values of τ which have symmetry we have non-generic behaviour. One can see that the point $b = (1 + \tau)/2$ is indeed a solution when $|\tau| = 1$, as discussed above.

The equations above simplify when we have only three edges in the field theory graph (which is to be drawn on the torus). Here, the dual graph has only one zero of order four, which we denote by z_0 , and the pole is at $b = 2z_0$. One can read off the constraint on the moduli space of marked tori from (105) with $\Delta z = 0$:

$$\zeta(z_0) - 2z_0\eta_1 + 2i\pi\text{Im}(z_0)/\tau_2 = 0. \quad (107)$$

Note that we have to look for solutions in which $b = 2z_0 \bmod (\text{lattice})$ is not a lattice point (since these do not correspond to Strebel differentials). This defines some two dimensional subspace of the moduli space, which we can analyze numerically. We observe that there are no solutions for $\tau = i$, for instance. In addition, for $\tau = e^{\pi i/3}$ one can see that $z_0 = (1 + e^{\pi i/3})/3$ and $z_0 = 2(1 + e^{\pi i/3})/3$ are solutions of equation (107), with $b = 2(1 + e^{\pi i/3})/3$ and $b = (1 + e^{\pi i/3})/3$, respectively¹⁵. These points appear in Figure 15(a) as the junction points where three lines meet. This is a general phenomenon: for all values of $\tau \neq i$ with $|\tau| = 1$ there are junctions of three lines which correspond to one edge going to zero length.

¹⁵Note that other values of z_0 for which $2z_0$ equals (modulo the lattice) these values of b are not solutions, so there is indeed a unique Strebel differential on a given marked Riemann surface.

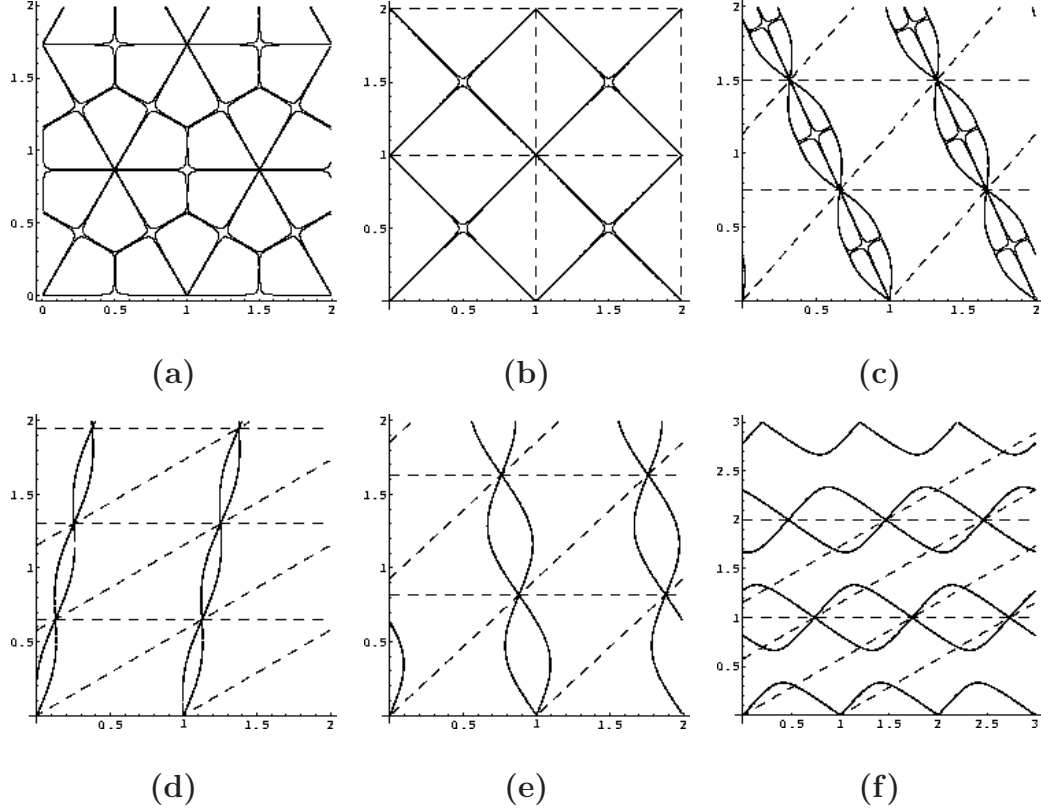


Figure 15: Numerical plots of the curves on which the second insertion, b , can lie for six different values of τ : **(a)** $\tau = e^{\pi i/3}$, **(b)** $\tau = i$, **(c)** $\tau = e^{i\pi/3.7}$, **(d)** $\tau = 1.3e^{i\pi/6}$, **(e)** $\tau = 1.2e^{i\pi/4.2}$, **(f)** $\tau = 2e^{i\pi/6}$. The fundamental domain is plotted with dashed lines (in figure (a) b can lie on the boundaries of the fundamental domain we chose). The small “diamonds” appearing in (a),(b),(c) are the result of numerical errors, and should be replaced by straight lines going through the middle of the “diamonds”.

Acknowledgements

We would like to thank O. Bergman, M. Berkooz, N. Itzhaki, Y. Oz, D. Reichmann, A. Schwimmer, and especially R. Gopakumar for useful discussions. The work of OA and ZK was supported in part by the Israel-U.S. Binational Science Foundation, by the Israel Science Foundation (grant number 1399/04), by the Braun-Roger-Siegl foundation, by the European network HPRN-CT-2000-00122, by a grant from the G.I.F., the German-Israeli Foundation for Scientific Research and Development, by Minerva, and by the Einstein center for theoretical physics. The work of SSR is supported in part by the Israel Science Foundation under grant no. 568/05.

Appendix

A More Sphere Diagrams

In this appendix we will discuss two additional sphere diagrams, the four-point and five-point diagrams with the topology of a circle (with edges running all around the circle). Such circular diagrams are the only contributions to correlation functions of the form $\langle \prod_{i=1}^n \text{Tr}(\Phi^2(x_i)) \rangle$. Our discussion will illustrate further some of the points which were mentioned in section 4. The four-point gauge theory diagram and dual critical graph are drawn in Figure 16. In the four-point diagram the decorated moduli space contains one modulus t and four circumferences; however, from the diagram it is clear that there is one linear relation between the circumferences (in the specific case drawn in Figure 16(b) it is $p_t + p_\infty = p_1 + p_{-t}$), so the diagram maps at most to a five-dimensional subspace of the decorated moduli space. However, in the gauge theory we have only four Schwinger parameters, so the diagram will localize on a codimension-one subspace of this five-dimensional subspace, similar to what we found in previous cases. In the case of the X amplitude which we discussed in section 4.4 the δ -function describing the localization did not depend on the magnitude of the complex modulus t (at leading order for small t), so the question of the leading power appearing in the OPE was well-defined. On the other hand, for the circle diagram we will see that the constraint does depend on $|t|$ even in the leading order, and thus we cannot determine the powers appearing in the OPE unless we explicitly

perform the integrals over the circumferences (which we were unable to do). In the case of the five-point circle diagram, we will see that the string theory diagram can be written without any δ -functions. We can translate explicitly all the circumferences to the string moduli (and one overall scaling parameter).

A.1 Circular four-point function

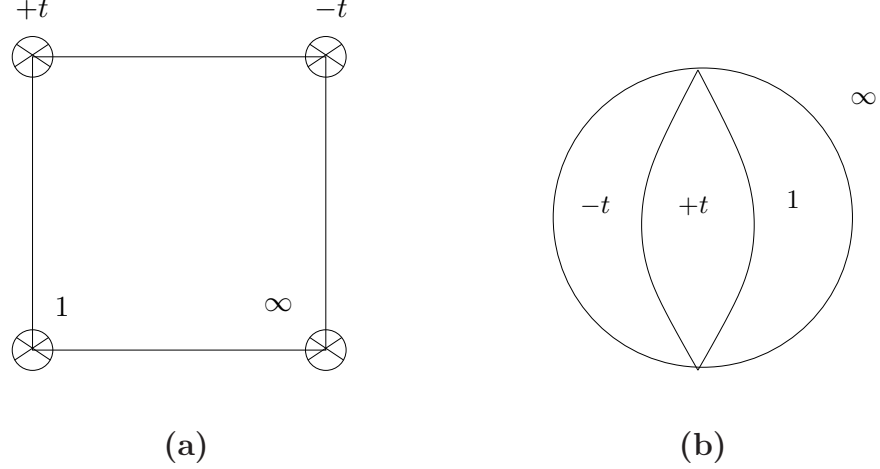


Figure 16: Four-point circle diagram on a sphere : **(a)** Gauge theory graph, **(b)** Dual graph.

The most general Strebel differential for the circular four-point diagram (with insertions at $z = 1, \pm t, \infty$) has the following form:

$$q = -\frac{1}{4\pi^2} \left(\gamma_+ \frac{p_t}{z-t} + \gamma_- \frac{p_{-t}}{z+t} + \gamma_1 \frac{p_1}{z-1} \right)^2 dz^2, \quad (108)$$

where the γ_i are sign choices which are determined by the ordering of the insertions around the circle. The ordering specifies a precise relation between the circumferences, which we wrote as $\gamma_+ p_t + \gamma_- p_{-t} + \gamma_1 p_1 = p_\infty$. In order to check that (108) is a Strebel differential we need to make sure that the edge-lengths are real. For given circumferences we will find one such condition, which implies that (for given circumferences) t cannot take any complex

value but lies in a one-dimensional subspace. The condition is :

$$\begin{aligned}
0 &= \text{Im}\left\{\int_{c_+}^{c_-} dz\sqrt{q}\right\} = \text{Re}\left\{\int_{c_+}^{c_-} \frac{dz}{2\pi}\left(\gamma_+\frac{p_t}{z-t} + \gamma_-\frac{p_{-t}}{z+t} + \gamma_1\frac{p_1}{z-1}\right)\right\} = \\
&= \frac{1}{2\pi}\text{Re}\left(\gamma_+p_t\ln(z-t) + \gamma_-p_{-t}\ln(z+t) + \gamma_1p_1\ln(z-1)\right)\Big|_{c_+}^{c_-},
\end{aligned} \tag{109}$$

where c_{\pm} are the two zeros of the differential; defining

$$B \equiv \frac{\gamma_+p_t + \gamma_-p_{-t}}{p_{\infty}}, \quad A \equiv \frac{\gamma_-p_{-t} - \gamma_+p_t}{p_{\infty}}, \tag{110}$$

they are given by:

$$c_{\pm} = \frac{1}{2}\left(B + At \pm \sqrt{(B + At)^2 - 4t(A + (B - 1)t)}\right). \tag{111}$$

Equation (109) is an explicit real constraint on the complex parameter t and on the real parameters A and B . A numerical solution of this constraint is depicted in Figure 17 for a specific value of t . The solutions $B(A, t)$ (or $A(B, t)$) scale with t even at the leading order

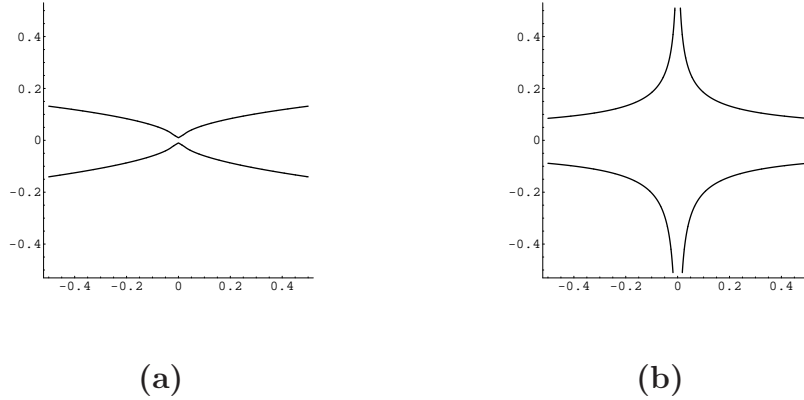


Figure 17: Solutions to the constraint (109), for a specific value $t = 0.0005e^{2.75i\pi}$: **(a)** This graph shows $B(A, t)$, **(b)** This graph shows $B(1/A, t)$. We see that the constraint can be solved to obtain as the three free real parameters the complex t and either A or B .

of small t . Thus, before solving the constraint and integrating over the circumferences (which we were not able to do) we cannot make any claim about the OPE arising from this diagram.

A.2 Circular five-point function

We turn now to the circular five-point diagram. The field theory and the dual graphs are very similar to the four-point case we discussed above. However, a crucial difference is that in this case there is no constraint relating the circumferences; in fact, there is a simple invertible linear relation between the five edge-lengths and the five circumferences. Choosing the insertions to lie at $z = 1, \pm t, b, \infty$, the general Strebel differential has the form:

$$q = \left(\frac{ip_\infty}{2\pi} \frac{(c_1 - z)^{3/2}(c_2 - z)^{3/2}}{(1 - z)(t^2 - z^2)(b - z)} dz \right)^2. \quad (112)$$

On the gauge theory side we have five Schwinger parameters; on the string theory side we have five independent circumferences and two complex moduli (t and b). Recalling that the moduli do not change when we rescale all the edges, we expect to be able to rewrite the gauge theory diagram as an integral over all the moduli and over an overall scale factor related to scaling all the circumferences. Namely, we expect that for any set of circumferences (up to rescalings) which is consistent with the topology of the graph, we will find a single value for the moduli.

The technical details are as follows. First, we change variables from the circumferences p_i to an overall scaling parameter p_∞ and four parameters α_i related to ratios of the circumferences, defined by :

$$\begin{aligned} \frac{p_1}{p_\infty} &= (-1)^{\gamma_1} \frac{(c_1 - 1)^{3/2}(c_2 - 1)^{3/2}}{(1 - t^2)(b - 1)} \equiv \alpha_1^{3/2}, \\ \frac{p_\pm}{p_\infty} &= (-1)^{\gamma_\pm} \frac{(c_1 \mp t)^{3/2}(c_2 \mp t)^{3/2}}{2t(1 \mp t)(b \mp t)} \equiv \alpha_\pm^{3/2}, \\ \frac{p_b}{p_\infty} &= (-1)^{\gamma_b} \frac{(c_1 - b)^{3/2}(c_2 - b)^{3/2}}{(t^2 - b^2)(1 - b)} \equiv \alpha_b^{3/2}. \end{aligned} \quad (113)$$

Here, we denoted the residues at $\pm t$ by p_\pm . The sign parameters γ_i take values in $\{0, 1\}$, according to which region of the parameter space we are in (as for the four-point function). The four complex equations (113) give a relation between the (real parameters) α_i , the two complex zero positions c_i and the two complex moduli. We would like to write the four circumference parameters α_i as functions of the moduli space. Define four quantities

which depend only on the moduli:

$$\begin{aligned}
F_{\pm} &\equiv e^{\frac{4\pi i}{3}\eta_{\pm} + \frac{2\pi i}{3}(1-\gamma_{\pm})} \left(2t(1 \mp t)(b \mp t) \right)^{2/3}, \\
F_b &\equiv e^{\frac{4\pi i}{3}\eta_b + \frac{2\pi i}{3}(1-\gamma_b)} \left((t^2 - b^2)(1 - b) \right)^{2/3}, \\
F_1 &\equiv e^{\frac{4\pi i}{3}\eta_1 + \frac{2\pi i}{3}(1-\gamma_1)} \left((t^2 - 1)(1 - b) \right)^{2/3},
\end{aligned} \tag{114}$$

where the η_i can take the values $\{0, 1, 2\}$ (assuming a specific choice of phase for the $2/3$ power). From the definition of α_{\pm} we find :

$$\begin{aligned}
c_1 c_2 &= \frac{1}{2} \left(\alpha_+ F_+ + \alpha_- F_- - 2t^2 \right), \\
c_1 + c_2 &= \frac{1}{2t} \left(-\alpha_+ F_+ + \alpha_- F_- \right).
\end{aligned} \tag{115}$$

Now, we have

$$\begin{aligned}
\alpha_b &= \frac{b^2 - t^2}{F_b} + \alpha_+ \left(1 + \frac{b}{t} \right) \frac{F_+}{2F_b} + \alpha_- \left(1 - \frac{b}{t} \right) \frac{F_-}{2F_b}, \\
\alpha_1 &= \frac{1 - t^2}{F_1} + \alpha_+ \left(1 + \frac{1}{t} \right) \frac{F_+}{2F_1} + \alpha_- \left(1 - \frac{1}{t} \right) \frac{F_-}{2F_1},
\end{aligned} \tag{116}$$

and we have two more equations which come from the reality of the circumferences:

$$\begin{aligned}
-\text{Im} \left(\frac{b^2 - t^2}{F_b} \right) &= \alpha_+ \text{Im} \left(\left(1 + \frac{b}{t} \right) \frac{F_+}{2F_b} \right) + \alpha_- \text{Im} \left(\left(1 - \frac{b}{t} \right) \frac{F_-}{2F_b} \right), \\
-\text{Im} \left(\frac{1 - t^2}{F_1} \right) &= \alpha_+ \text{Im} \left(\left(1 + \frac{1}{t} \right) \frac{F_+}{2F_1} \right) + \alpha_- \text{Im} \left(\left(1 - \frac{1}{t} \right) \frac{F_-}{2F_1} \right).
\end{aligned} \tag{117}$$

We can now write α_{\pm} purely as a function of the circumferences :

$$\begin{aligned}
\frac{1}{2}\alpha_+ &= \frac{-\text{Im} \left[\frac{b^2 - t^2}{F_b} \right] \text{Im} \left[\left(1 - \frac{1}{t} \right) \frac{F_-}{F_1} \right] + \text{Im} \left[\frac{1 - t^2}{F_1} \right] \text{Im} \left[\left(1 - \frac{b}{t} \right) \frac{F_-}{F_b} \right]}{\text{Im} \left[\left(1 + \frac{b}{t} \right) \frac{F_+}{F_b} \right] \text{Im} \left[\left(1 - \frac{1}{t} \right) \frac{F_-}{F_1} \right] - \text{Im} \left[\left(1 + \frac{1}{t} \right) \frac{F_+}{F_1} \right] \text{Im} \left[\left(1 - \frac{b}{t} \right) \frac{F_-}{F_b} \right]}, \\
\frac{1}{2}\alpha_- &= \frac{\text{Im} \left[\frac{b^2 - t^2}{F_b} \right] \text{Im} \left[\left(1 + \frac{1}{t} \right) \frac{F_+}{F_1} \right] - \text{Im} \left[\frac{1 - t^2}{F_1} \right] \text{Im} \left[\left(1 + \frac{b}{t} \right) \frac{F_+}{F_b} \right]}{\text{Im} \left[\left(1 + \frac{b}{t} \right) \frac{F_+}{F_b} \right] \text{Im} \left[\left(1 - \frac{1}{t} \right) \frac{F_-}{F_1} \right] - \text{Im} \left[\left(1 + \frac{1}{t} \right) \frac{F_+}{F_1} \right] \text{Im} \left[\left(1 - \frac{b}{t} \right) \frac{F_-}{F_b} \right]}.
\end{aligned} \tag{118}$$

Thus, we have found explicitly the dictionary from the moduli to the ratios of the circumferences. We can calculate the Jacobian in a straightforward way, though the explicit

expression is quite complicated. The only things which are not set yet are the phases γ_i and η_i ; this is a discrete choice of parameters, depending on which region of the moduli space we are in. The exact regions are not simple to compute, but we will mostly be interested in the OPE region $t \rightarrow 0$ where we will be able to determine the phases.

The gauge theory result for a five-point function $\langle \prod_{i=1}^5 \text{Tr}(\Phi^{J_i}(x_i)) \rangle$ is given by:

$$G \propto \int \left(\prod_{i=1}^5 d\sigma_i \sigma_i^{m_i-1} \right) e^{-\frac{(x_1-x_2)^2 \sigma_1}{4} - \frac{(x_2-x_3)^2 \sigma_2}{4} - \frac{(x_3-x_4)^2 \sigma_3}{4} - \frac{(x_4-x_5)^2 \sigma_4}{4} - \frac{(x_5-x_1)^2 \sigma_5}{4}}, \quad (119)$$

where the m_i are related in a simple way to the J_i . There is a similar simple relation between the σ_i and the circumferences p_i (written in a specific ordering depending on the ordering of the vertices around the graph). Defining $\beta_i \equiv p_i/p_\infty$, it is given by

$$\sigma_i = \frac{1}{2} \sum_{k=0}^4 (-1)^k p_{i+k \pmod{5}} = \frac{1}{2} p_\infty \sum_{k=0}^4 (-1)^k \beta_{i+k \pmod{5}}. \quad (120)$$

We can now change coordinates from the σ_i to four β_i and p_∞ . The Jacobian is proportional to p_∞^4 . Defining

$$G_2(\beta) = \frac{(x_1-x_2)^2 \sigma_1 + (x_2-x_3)^2 \sigma_2 + (x_3-x_4)^2 \sigma_3 + (x_4-x_5)^2 \sigma_4 + (x_5-x_1)^2 \sigma_5}{4p_\infty} \quad (121)$$

(which is implicitly a function of the β 's using (120)), the amplitude becomes:

$$\begin{aligned} G &\propto \int_0^\infty dp_\infty p_\infty^{4+\sum_{i=1}^5 (m_i-1)} \int_0^\infty \prod_{i=1}^4 d\beta_i \left[\prod_{j=1}^5 \left(\frac{1}{2} \sum_{k=0}^4 (-1)^k \beta_{j+k} \right)^{m_j-1} \right] e^{-p_\infty G_2(\beta)} \quad (122) \\ &\propto \int_0^\infty \prod_{i=1}^4 d\beta_i \frac{G_1(\beta)}{(G_2(\beta))^{\sum_{i=1}^5 m_i}}, \end{aligned}$$

where

$$G_1(\beta) \equiv \prod_{j=1}^5 \left(\frac{1}{2} \sum_{k=0}^4 (-1)^k \beta_{j+k} \right)^{m_j-1}. \quad (123)$$

Above we calculated the dictionary between the $\alpha_i = \beta_i^{2/3}$ and the moduli t, b , so we can now rewrite (122) as a (complicated) integral over the moduli.

All that remains to compute the OPE is to analyze the choice of phases η_i, γ_i . We assume that the points $\pm t$ lie in adjacent disks of the critical graph; specifically, we choose

the cyclic order of the points to be $t, -t, 1, b, \infty$. For a “generic” choice of signs, with different signs at t and $-t$, we find that as $t \rightarrow 0$ $\alpha_{\pm} \sim |t|^{1/3}$ and $\alpha_{b,1} \sim |t|^0$, which implies that $\beta_{\pm} \sim \sqrt{|t|}$ and $\beta_{b,1}$ are finite. Since each circumference p_i is the sum of two adjacent σ ’s, this means that three σ_i ’s go as $\sqrt{|t|}$ and two go as $|t|^0$. We claim that this case is inconsistent. If we have three edges going to zero then we should have that (at leading order in t) $p_b = p_1 + p_{\infty}$, or $\alpha_b^{3/2} = \alpha_1^{3/2} + 1$. In the limit of $t \rightarrow 0$ we have:

$$F_{\pm} = \delta_{\pm} \left(2tb \right)^{2/3}, \quad F_b = \delta_b \left(b^2(1-b) \right)^{2/3}, \quad F_1 = \delta_1 \left(1-b \right)^{2/3}, \quad (124)$$

and

$$\begin{aligned} 2\alpha_b &= \frac{2b^2}{F_b} + \left(F_+ \alpha_+ - F_- \alpha_- \right) \frac{b}{tF_b}, \\ 2\alpha_1 &= \frac{2}{F_1} + \left(F_+ \alpha_+ - F_- \alpha_- \right) \frac{1}{tF_1}. \end{aligned} \quad (125)$$

The only solution we could find to¹⁶ $\alpha_b^{3/2} = \alpha_1^{3/2} + 1$ is to choose $\delta_+ = \delta_-$; in this case at leading order we have $F_+ = F_-$ and $\alpha_+ = \alpha_-$ so $F_+ \alpha_+ - F_- \alpha_- = 0$, and then

$$\alpha_b^{3/2} - \alpha_1^{3/2} = \left(\frac{b^3}{\delta_b^{3/2} b^2(1-b)} - \frac{1}{\delta_1^{3/2}(1-b)} \right), \quad (126)$$

which indeed equals one for an appropriate choice of δ_b, δ_1 .

However, in this case of $\delta_+ = \delta_-$ it actually turns out that the scaling at small t is different. In this case we find $\alpha_{\pm} \sim |t|^{-2/3}$ and $\alpha_{b,1} \sim |t|^0$, which implies that $\beta_{\pm} \sim 1/|t|$ and $\beta_{b,1} \sim 1$. Thus, one of the σ_i ’s (the edge connecting the two operators which are coming together) scales as $1/|t|$ while the others are finite (as we found in some of the previous OPEs we analyzed). The Jacobian for the change of variables from the β ’s to the absolute value and phase of t and b goes in this case as $A/|t|^2 + B/|t|$ for some constants A and B . It is easy to see that $G_1 \propto |t|^{1-\frac{1}{2}(J_t+J_{-t}-J_1+J_b-J_{\infty})}$ while $G_2 \propto (x_t - x_{-t})^2/|t|$, so we find that the full diagram scales as (for small t)

$$\begin{aligned} G &\propto \int d|t| d(\arg(t)) \frac{1}{|t|^2} |t|^{1-\frac{1}{2}(J_t+J_{-t}-J_1+J_b-J_{\infty})} (|t|/(x_t - x_{-t})^2)^{\sum_i m_i} \\ &\propto \int d^2 t |t|^{J_1+J_{\infty}-2} |x_t - x_{-t}|^{-\sum_i J_i}. \end{aligned} \quad (127)$$

¹⁶We can prove this is the only solution in some regions of parameter space, such as $1/|t| \gg |b| \gg 1$.

It is easy to see that whenever the diagram is non-zero, the power of t that we find is always larger than the power we found in the *star* diagrams which was $|J_t - J_{-t}| - 2$. So, the OPE is consistent with this being the minimal power appearing in the OPE, and we see that in many cases in the five-point function all the leading terms in the OPE cancel and the first term appearing is (127). The space-time dependence of the leading small t result is again consistent with scaling invariance.

B A Short Primer on Elliptic Functions

In our study of Strebel differentials on a torus we need to use elliptic functions. In this section we will briefly review the basic theory of such functions and some useful facts. A meromorphic function $f(z)$ which is doubly periodic,

$$f(z + a) = f(z + \tilde{a}) = f(z), \quad (128)$$

where the periods satisfy $\text{Im}(\tilde{a}/a) > 0$, is called an elliptic function. These functions have many nice properties, including :

- The sum of the residues of the simple poles of an elliptic function inside the period-parallelogram (the parallelogram spanned by the two periods a and \tilde{a}) is equal to zero.
- The number of zeros of a non-constant elliptic function inside the period parallelogram is equal to the number of poles, where the zeros and poles are weighted by their degrees.
- The sum of the positions of the zeros of a non-constant elliptic function inside the period parallelogram differs from the sum of the position of the poles by a period (an integer linear combination of a and \tilde{a}), where again the sum is weighted by the degrees of the zeros and poles.

A useful example of an elliptic function is the Weierstrass function, which can be defined by the following expansion:

$$\wp(z|\tau) = \frac{1}{z^2} + \sum_{m,n \neq (0,0)} \left(\frac{1}{(z + m + n\tau)^2} - \frac{1}{(m + n\tau)^2} \right). \quad (129)$$

This is a periodic function with periods τ and 1 and with a double pole at $z = 0$. This function solves the following differential equation:

$$\wp'(z|\tau)^2 = 4(\wp(z|\tau) - e_1)(\wp(z|\tau) - e_2)(\wp(z|\tau) - e_3), \quad e_1 + e_2 + e_3 = 0 \quad (130)$$

where the derivative is with respect to z , $e_i \equiv \wp(\omega_i)$ and ω_i are the half-periods of the torus,

$$\omega_1 = \frac{1}{2}, \quad \omega_2 = \frac{1+\tau}{2}, \quad \omega_3 = \frac{\tau}{2}. \quad (131)$$

Another useful property of this function is the addition theorem:

$$\wp(z_1 + z_2) = \frac{1}{4} \left(\frac{\wp'(z_1) - \wp'(z_2)}{\wp(z_1) - \wp(z_2)} \right)^2 - \wp(z_1) - \wp(z_2). \quad (132)$$

Any elliptic function $f(z|\tau)$ can be written as:

$$f(z|\tau) = P(\wp(z|\tau)) + \wp'(z|\tau)Q(\wp(z|\tau)) \quad (133)$$

where $P(x)$ and $Q(x)$ are rational functions. From the properties we quoted above it follows that if one is given the structure of singularities of a given elliptic function, and one succeeds in building another elliptic function with the same singularities, the two functions will differ by a constant. We will use this fact extensively.

There are some additional functions related to the Weierstrass function, which are not elliptic but nevertheless play an important role. We define $\sigma(z)$ and $\zeta(z)$ by their relation to the Weierstrass $\wp(z)$ function,

$$\frac{\sigma'(z)}{\sigma(z)} = \zeta(z), \quad \zeta'(z) = -\wp(z). \quad (134)$$

A useful identity for $\sigma(z)$ is its variation along the periods of the torus

$$\sigma(z + 2\omega_i) = -e^{2\eta_i(z+\omega_i)}\sigma(z), \quad (135)$$

where $\eta_i \equiv \zeta(\omega_i)$. We will also use the Legendre theorem, which states that for the periods $(2\omega_1, 2\omega_3) = (1, \tau)$

$$\tau\eta_1 - \eta_3 = i\pi. \quad (136)$$

References

- [1] G. 't Hooft, “A planar diagram theory for strong interactions,” Nucl. Phys. B **72**, 461 (1974).
- [2] J. M. Maldacena, “The large N limit of superconformal field theories and supergravity,” Adv. Theor. Math. Phys. **2**, 231 (1998) [Int. J. Theor. Phys. **38**, 1113 (1999)] [arXiv:hep-th/9711200]; S. S. Gubser, I. R. Klebanov and A. M. Polyakov, “Gauge theory correlators from non-critical string theory,” Phys. Lett. B **428** (1998) 105 [arXiv:hep-th/9802109]; E. Witten, “Anti-de Sitter space and holography,” Adv. Theor. Math. Phys. **2**, 253 (1998) [arXiv:hep-th/9802150].
- [3] R. Gopakumar and C. Vafa, “On the gauge theory/geometry correspondence,” Adv. Theor. Math. Phys. **3**, 1415 (1999) [arXiv:hep-th/9811131]; H. Ooguri and C. Vafa, “Worldsheet derivation of a large N duality,” Nucl. Phys. B **641**, 3 (2002) [arXiv:hep-th/0205297].
- [4] B. Sundborg, “The Hagedorn transition, deconfinement and N = 4 SYM theory,” Nucl. Phys. B **573**, 349 (2000) [arXiv:hep-th/9908001]; O. Aharony, J. Marsano, S. Minwalla, K. Papadodimas and M. Van Raamsdonk, “The Hagedorn / deconfinement phase transition in weakly coupled large N gauge theories,” Adv. Theor. Math. Phys. **8**, 603 (2004) [arXiv:hep-th/0310285].
- [5] K. Bardakci and C. B. Thorn, “A worldsheet description of large N_c quantum field theory,” Nucl. Phys. B **626**, 287 (2002) [arXiv:hep-th/0110301]; C. B. Thorn, “A worldsheet description of planar Yang-Mills theory,” Nucl. Phys. B **637**, 272 (2002) [Erratum-ibid. B **648**, 457 (2003)] [arXiv:hep-th/0203167]; K. Bardakci and C. B. Thorn, “A mean field approximation to the world sheet model of planar ϕ^3 field theory,” Nucl. Phys. B **652**, 196 (2003) [arXiv:hep-th/0206205]; S. Gudmundsson, C. B. Thorn and T. A. Tran, “BT worldsheet for supersymmetric gauge theories,” Nucl. Phys. B **649**, 3 (2003) [arXiv:hep-th/0209102]; K. Bardakci and C. B. Thorn, “An improved mean field approximation on the worldsheet for planar ϕ^3 theory,” Nucl. Phys. B **661**, 235 (2003) [arXiv:hep-th/0212254]; C. B. Thorn and T. A. Tran, “The

- fishnet as anti-ferromagnetic phase of worldsheet Ising spins,” Nucl. Phys. B **677**, 289 (2004) [arXiv:hep-th/0307203]; K. Bardakci, “Further results about field theory on the world sheet and string formation,” Nucl. Phys. B **715** (2005) 141 [arXiv:hep-th/0501107].
- [6] P. Haggi-Mani and B. Sundborg, “Free large N supersymmetric Yang-Mills theory as a string theory,” JHEP **0004** (2000) 031 [arXiv:hep-th/0002189]; H. L. Verlinde, “Bits, matrices and $1/N$,” JHEP **0312** (2003) 052 [arXiv:hep-th/0206059]; J. G. Zhou, “pp-wave string interactions from string bit model,” Phys. Rev. D **67** (2003) 026010 [arXiv:hep-th/0208232]; D. Vaman and H. L. Verlinde, “Bit strings from $N = 4$ gauge theory,” JHEP **0311** (2003) 041 [arXiv:hep-th/0209215]; A. Dhar, G. Mandal and S. R. Wadia, “String bits in small radius AdS and weakly coupled $N = 4$ super Yang-Mills theory. I,” arXiv:hep-th/0304062; K. Okuyama and L. S. Tseng, “Three-point functions in $N = 4$ SYM theory at one-loop,” JHEP **0408** (2004) 055 [arXiv:hep-th/0404190]; L. F. Alday, J. R. David, E. Gava and K. S. Narain, “Structure constants of planar $N = 4$ Yang Mills at one loop,” JHEP **0509** (2005) 070 [arXiv:hep-th/0502186]; J. Engquist and P. Sundell, “Brane partons and singleton strings,” arXiv:hep-th/0508124; L. F. Alday, J. R. David, E. Gava and K. S. Narain, “Towards a string bit formulation of $N = 4$ super Yang-Mills,” arXiv:hep-th/0510264.
- [7] J. Polchinski, unpublished.
- [8] A. Karch, “Lightcone quantization of string theory duals of free field theories,” arXiv:hep-th/0212041; A. Clark, A. Karch, P. Kovtun and D. Yamada, “Construction of bosonic string theory on infinitely curved anti-de Sitter space,” Phys. Rev. D **68**, 066011 (2003) [arXiv:hep-th/0304107].
- [9] G. Bonelli, “On the boundary gauge dual of closed tensionless free strings in AdS,” JHEP **0411** (2004) 059 [arXiv:hep-th/0407144].
- [10] N. Itzhaki and J. McGreevy, “The large N harmonic oscillator as a string theory,” Phys. Rev. D **71** (2005) 025003 [arXiv:hep-th/0408180].

- [11] R. Gopakumar, “From free fields to AdS,” Phys. Rev. D **70**, 025009 (2004) [arXiv:hep-th/0308184]; R. Gopakumar, “From free fields to AdS. II,” Phys. Rev. D **70**, 025010 (2004) [arXiv:hep-th/0402063]; R. Gopakumar, “Free field theory as a string theory?,” Comptes Rendus Physique **5**, 1111 (2004) [arXiv:hep-th/0409233]; R. Gopakumar, “From free fields to AdS. III,” Phys. Rev. D **72**, 066008 (2005) [arXiv:hep-th/0504229].
- [12] M. Bianchi, J. F. Morales and H. Samtleben, “On stringy AdS(5) x S⁵ and higher spin holography,” JHEP **0307** (2003) 062 [arXiv:hep-th/0305052]; N. Beisert, M. Bianchi, J. F. Morales and H. Samtleben, “On the spectrum of AdS/CFT beyond supergravity,” JHEP **0402** (2004) 001 [arXiv:hep-th/0310292].
- [13] E. T. Akhmedov, “Expansion in Feynman graphs as simplicial string theory,” JETP Lett. **80**, 218 (2004) [Pisma Zh. Eksp. Teor. Fiz. **80**, 247 (2004)] [arXiv:hep-th/0407018].
- [14] K. Furuuchi, “From free fields to AdS: Thermal case,” Phys. Rev. D **72** (2005) 066009 [arXiv:hep-th/0505148].
- [15] B. Zwiebach, “Closed string field theory: Quantum action and the B-V master equation,” Nucl. Phys. B **390**, 33 (1993) [arXiv:hep-th/9206084]; A. Belopolsky and B. Zwiebach, “Off-shell closed string amplitudes: Towards a computation of the tachyon potential,” Nucl. Phys. B **442**, 494 (1995) [arXiv:hep-th/9409015].
- [16] N. Moeller, “Closed bosonic string field theory at quartic order,” JHEP **0411** (2004) 018 [arXiv:hep-th/0408067].
- [17] K. Strebel, “Quadratic differentials,” Springer-Verlag, 1984.
- [18] M. Mulase, M. Penkava, “Ribbon graphs, quadratic differentials on Riemann surfaces, and algebraic curves defined over $\bar{\mathbb{Q}}$,” [math-ph/9811024].
- [19] D. Zvonkine, “Strebel differentials on stable curves and Kontsevich’s proof of Witten’s conjecture,” [math.AG/0209071].

- [20] M. Kontsevich, “Intersection theory on the moduli space of curves and the matrix Airy function,” *Commun. Math. Phys.* **147**, 1 (1992); E. Witten, “Two-dimensional gravity and intersection theory on moduli space,” *Surveys Diff. Geom.* **1**, 243 (1991).
- [21] J. Teschner, “On structure constants and fusion rules in the $SL(2,C)/SU(2)$ WZNW model,” *Nucl. Phys. B* **546**, 390 (1999) [arXiv:hep-th/9712256]; J. Teschner, “The mini-superspace limit of the $SL(2,C)/SU(2)$ WZNW model,” *Nucl. Phys. B* **546**, 369 (1999) [arXiv:hep-th/9712258]; J. Teschner, “Operator product expansion and factorization in the H_3^+ WZNW model,” *Nucl. Phys. B* **571**, 555 (2000) [arXiv:hep-th/9906215]; J. Teschner, “Crossing symmetry in the H_3^+ WZNW model,” *Phys. Lett. B* **521**, 127 (2001) [arXiv:hep-th/0108121].
- [22] J. M. Maldacena and H. Ooguri, “Strings in $AdS(3)$ and $SL(2,R)$ WZW model. I,” *J. Math. Phys.* **42**, 2929 (2001) [arXiv:hep-th/0001053]; J. M. Maldacena, H. Ooguri and J. Son, “Strings in $AdS(3)$ and the $SL(2,R)$ WZW model. II: Euclidean black hole,” *J. Math. Phys.* **42**, 2961 (2001) [arXiv:hep-th/0005183]; J. M. Maldacena and H. Ooguri, “Strings in $AdS(3)$ and the $SL(2,R)$ WZW model. III: Correlation functions,” *Phys. Rev. D* **65**, 106006 (2002) [arXiv:hep-th/0111180].
- [23] A. Giveon, D. Kutasov and O. Pelc, “Holography for non-critical superstrings,” *JHEP* **9910** (1999) 035 [arXiv:hep-th/9907178]; A. Giveon and D. Kutasov, “Little string theory in a double scaling limit,” *JHEP* **9910** (1999) 034 [arXiv:hep-th/9909110]; A. Giveon and D. Kutasov, “Comments on double scaled little string theory,” *JHEP* **0001** (2000) 023 [arXiv:hep-th/9911039].
- [24] D. Kutasov and N. Seiberg, “More comments on string theory on $AdS(3)$,” *JHEP* **9904** (1999) 008 [arXiv:hep-th/9903219].
- [25] N. R. Constable, D. Z. Freedman, M. Headrick, S. Minwalla, L. Motl, A. Postnikov and W. Skiba, “PP-wave string interactions from perturbative Yang-Mills theory,” *JHEP* **0207** (2002) 017 [arXiv:hep-th/0205089].